∼ Bending the Waves –

Detrending and Forecasting Intraday Stock Volatility*

Martin Haas† & Benedikt Schmehr‡

Zeppelin University, Friedrichshafen

July 15, 2019

Abstract

In this paper we examine the volatility forecasting performance for intraday returns, after filtering out a deterministic periodic pattern with two different approaches. In essence, we employ a parametric approach based on Fourier flexible form as well as a non-parametric approach to estimate and filter out the intraday pattern in absolute 5-minute returns. Using the filtered returns we then perform volatility forecasts with standard GARCH(1,1) models. our findings support the view that the non-parametric approach might be more suitable for one-step-ahead intraday volatility forecasts.

Keywords: Intraday, Volatility, Forecasting, Fourier Flexible Form

1 Introduction

All financial institutions, like banks, funds or exchanges, require adequate information and procedures to manage the financial transactions that are carried out on a daily basis. Besides monitoring the extreme multitude of activities on their own accord, they also have to conform with a range of regulatory requirements, e.g. from the Basle Committee on Banking Supervision. For frequently traded assets, measures of financial risk are arguably amongst the most important informational factors. Described by asset return volatility, risk finds its use in portfolio construction, e.g. in the CAPM, despite its known deficits (for an overview and discussion see Fama and French 2004). When the future risk of an investment loss is assessed through

*Zeppelin University, Friedrichshafen — We thank our supervisors *(i)* Prof. Dr. Franziska Peter, *Chair of Empirical Finance and Econometrics, Zeppelin University* and *(ii)* Simon Behrendt MSc.

†m.haas@zeppelin-university.net

‡b.schmehr@zeppelin-university.net

Value-at-Risk (see Alexander 2008) or when options are priced utilizing the (in)famous Black-Scholes Option Pricing Model (Black and Scholes 1973), forecasts of volatility are needed as input variables. Known and obvious shortcomings in the aforementioned and still widely used models are a major driver of the continual research in these specific areas.

With the advent of high frequency trading and rising availability of data, the frequency in which volatility is and needs to be assessed has increased gradually. Initially observed only on the *inter*daily level, state-of-the-art research now focuses on the *intra*daily level with recording accuracy up to each individual trade. However, high-frequency data exhibits several features, also termed as *market micro-structure noise*, which render volatility estimates and the use of models developed for *inter*daily data inadequate (Poon and Granger 2003). This micro-structure noise is due to effects like the bid-ask bounce and sampling methods that make up for infrequent and non-synchronous trading (see e.g. Hansen and Lunde 2006) or human error and competition between traders (Zhou 1996). However, the distorting effects of this noise on the actual informational content can be mitigated by using lower sampling frequencies, e.g. five or twenty minutes (Hansen and Lunde 2006). An additional phenomenon attributed to human behaviour is the intraday periodic pattern of volatility: when observing stock volatility over the trading day, one finds a reoccurring pattern of relatively high volatility at the opening and closing of exchanges and low volatility around the lunch hours (c.f. Behrendt and Schmidt 2018; Andersen and Bollerslev 1997). This wavelike periodicity can be observed every when looking at volatility over several days, even when lower frequencies are employed. This pattern and methods to "treat" it in order to model and forecast volatility more accurately are the focus of this paper. The findings of this paper therefore might especially be interesting for high-frequency traders or investors, who need to access sophisticated volatility estimates as well as forecasts on a higher than daily frequency.

We examine two different approaches to recover the "true" intraday volatility. In order to do so, intraday returns are decomposed into multiplicative components including a volatility factor and a periodic component. The first approach, employed by e.g. Behrendt and Schmidt (2018) and developed by Andersen and Bollerslev (1997) uses a semi-parametric curve-fitting method based on the Fourier Flexible Form ("FFF-Regression"), while the second approach by R. F. Engle and Sokalska (2012) and Taylor and Xu (1997) uses a non-parametric sample variance estimator. We apply both methods to estimate the periodic (intraday) volatility component, which then can be filtered out of the returns. We then use the filtered returns to forecast intraday volatility and asses the forecast evaluation in order to determine which method is best suited to perform this task. Both procedures require the input of

a daily volatility factor, which we estimate using the A-PARCH model by Ding et al. (1993) and a dataset of daily closing prices.

Our findings support the view that one-step-ahead volatility forecasting endeavours, based on a 5-minute intraday frequency using a series of filtered returns and standard GARCH(1,1) models should favour the non-parametric approach by Taylor and Xu (1997) over the semi-parametric FFF-Regression as a method to estimate and filter out the periodic volatility component, even when allowing for a multitude of possible tuning parameters in the latter.

The remainder of this paper will be structured as follows. In section 2 we give an introduction to the literature which previously covered the topic of the intraday periodic component. Section 3 provides an overview of the two datasets which will be used in this paper. The return decomposition model, the two trend estimation models as well as the filtering procedure are described in section 4 and the corresponding results in section 5. Section 6 describes the forecast modelling and bench-marking approach and reports the results accordingly. We discuss and conclude in section 7.

2 Literature review

The earliest recognitions of the intraday periodic pattern date back to the 1980s, when the first research on intraday trading became possible with the uprising of electronic trading in the previous decade. Before that, a distinct interdaily pattern in stock returns was already known and observed, e.g. in daily closing and midday prices (c.f. Harris (1986)). One of the earliest studies on seasonality on the intraday level is represented by the seminal paper of Wood et al. (1985), who find patterns in the absolute returns[1] and autocorrelations of trades on the New York Stock Exchange (NYSE). Jain and Joh (1988), who cover the same exchange, additionally found that absolute returns vary over the day and are asymmetrically related to the trading volume, i.e. the relation significantly differs depending on the sign of the returns. Generally it can be said that volatility is not only influenced by inherent properties of stocks and buyer's or seller's preferences and requirements, but also by the structure of the market with its limited trading hours. This turns out to be more clear when foreign exchange markets are analysed as they are generally open twenty-four seven. Repeating patterns of higher trading activities can be observed in these markets, depending on the opening and lunch hours of exchanges all around the world (see e.g. Bollerslev and Domowitz (1993), Müller et al. (1990), and Hecq et al. (2012)). As Dacorogna et al. (1993) put it, observing intradaily instead of interdaily data allows "us to tackle a fundamental source of seasonality, the revolution of the earth." As traders start and end their days or take lunch breaks, activity rises and

[1] Absolute returns are used as a proxy for volatility, since they exhibit desirable properties. For a broad overview see for instance Poon and Granger (2003, p. 480) and Ding et al. (1993)

falls around the globe, leading to the wave-like patterns that gave rise to the title of this paper. But, as Baillie and Bollerslev (1991) hint, the seasonality is not simply due to human needs like sleep and sustenance, but also to strategic trader interactions.

Admati and Pfleiderer (1988) construct a model which divides traders into information and liquidity traders. While the former trade on exclusive information on an asset in order to generate a profit, the latter trade for other reasons that are not necessarily related to future payoffs. They show that, if liquidity (or also "noise") traders have discretion over the time at which they execute their trades, they tend to generally concentrate and also cluster close to periods at which they need to realize their demands. Information traders are found to trade in periods of high activity, and thus increase this effect even more.

The higher activity observed at the opening and closing of exchanges can now be explained by higher activity of non-discretionary liquidity trades, which need to be realised as soon as possible – which then attracts the activity of discretionary liquidity and information traders. This behaviour induces the observed U-shaped pattern. Since it is created partly by noise-traders, its informational content is limited – it is an essentially deterministic trend due to the market structure. With the goal to utilise the additional information that intraday data yields with respect to daily data, this pattern becomes problematic, as it additionally violates crucial model assumptions.

This is the case for the application of standard ARMA or GARCH-type models. In their seminal paper, Andersen and Bollerslev (1997) make the clear point that "standard ARCH models imply a geometric decay in the return autocorrelation structure and simply cannot accommodate strong regular cyclical patterns." In order to use these models, this pattern needs to be accounted for. The most basic approach is to include intraday dummy variables as suggested in Baillie and Bollerslev (1991). More sophisticated approaches decompose returns into a daily variance, an intraday variance and a seasonal component. The latter is then estimated and filtered out, either via a parametric or non-parametric technique. Examples of the former approach include the framework of Andersen and Bollerslev (1997) and Andersen and Bollerslev (1998), who use a series of trigonometric terms to approximate the wave-like pattern, called the "Fourier flexible form" or FFF-Regression. As one of the most popular approaches, it has been widely applied in empirical work and was even extended to be robust to jumps (Boudt et al. 2008) and accomodated to the multivariate domain (Hecq et al. 2012). The alternative non-parametric approaches use a simple variance estimator to estimate the seasonal component, e.g. Taylor and Xu (1997) and R. F. Engle and Sokalska (2012), which we will further be referred to as the "TX-Estimator".

With both the FFF and the TX-Method, the described wave-pattern can be estimated

and filtered out of the intraday data, facilitating the analysis of its "real" informational content. However, it is not yet clear which approach yields the best results to this task, which of course also depends on the specific task at hand. In order to shed some light on this specific topic, we employ both methods to remove the U-shaped pattern and then measure the performance of volatility forecasts, which are a very common and important tool in the financial sector.

3 Data

Our initial intraday dataset consists of 7 stocks and covers the period from February 1st, 2017 to March 31st, 2017 for both the NYSE and NASDAQ on a 1-second frequency. Prices are recorded as midquotes, which are assumed to reduce the bid-ask bounce effect as suggested by Robert F. Engle (2000, p. 16) and Brownlees and Gallo (2006, p. 2239). We calculate the continuously compounded returns as the log-price changes from one second to the following, i.e.

$$r_i = \ln(p_i) - \ln(p_{i-1}). \tag{1}$$

Additionally, we remove outliers from this sample, which we define as returns for which their absolute value is larger than 25 times the standard deviation of the series. These outliers are assumed to be data errors common in unfiltered intraday stock price data. We report the summary statistics of the returns in Table 1, which after the removal of the outliers are consistent and comparable over both stock exchanges. As the effects of market-microstructure noise dominate the informational content in returns as the sampling frequency increases (Hansen and Lunde 2006; Zhou 1996), we aggregate the initial return series to a lower frequency by calculating the 5-minute returns as the sum of three hundred consecutive 1-second returns. Excluding the overnight-returns following R. F. Engle and Sokalska (2012, p. 57), this leaves us with $N = 77$ intraday "bins" and $T = 42$ days, resulting in a total of $NT = 3234$ observations per stock and exchange. The 5-minute returns are then denoted as $R_{t,n}$, with $n = 1, 2, \ldots, N$ and $t = 1, 2, \ldots, T$. Figure 1a shows that our data clearly exhibits the typical intraday pattern in the absolute 5-minute returns, $|R_{t,n}|$. Likewise, the autocorrelation functions of each stock also show the wave-like pattern, as it can be examined in Figure 1b, as well as in the Appendix for the remaining stocks.

Our second dataset, containing the daily stock prices of the observed 7 stocks, is obtained from Yahoo! Finance using the `quantmod` package in `R` and is used to calculate the daily volatility proxy for the two-step estimation procedure described below. Following Behrendt and Schmidt 2018, we obtain data from January 4th, 2010 until December 29th, 2017 and thus excluding the recent financial crisis.

Ticker	min	mean	max	SD
NASDAQ				
JNJ	-0.1412%	0.0000139%	0.1368%	0.00402%
JPM	-0.1162%	0.0000000%	0.1317%	0.00569%
PG	-0.1365%	0.0000042%	0.1423%	0.00380%
T	-0.1319%	0.0000032%	0.1420%	0.00447%
WFC	-0.1275%	-0.0000003%	0.1398%	0.00634%
WMT	-0.1420%	0.0000020%	0.1327%	0.00539%
XOM	-0.1344%	0.0000008%	0.1380%	0.00470%
NYSE				
JNJ	-0.1424%	0.0000143%	0.1374%	0.00386%
JPM	-0.1379%	-0.0000008%	0.1044%	0.00560%
PG	-0.1315%	0.0000042%	0.1097%	0.00370%
T	-0.1323%	0.0000029%	0.1420%	0.00445%
WFC	-0.1202%	-0.0000011%	0.1188%	0.00630%
WMT	-0.1350%	0.0000020%	0.1254%	0.00525%
XOM	-0.1348%	0.0000008%	0.1320%	0.00458%

Table 1: *Summary statistics for the intraday stock returns. The observed time series ranges from February 1st, 2017 to March 31st, 2017.*

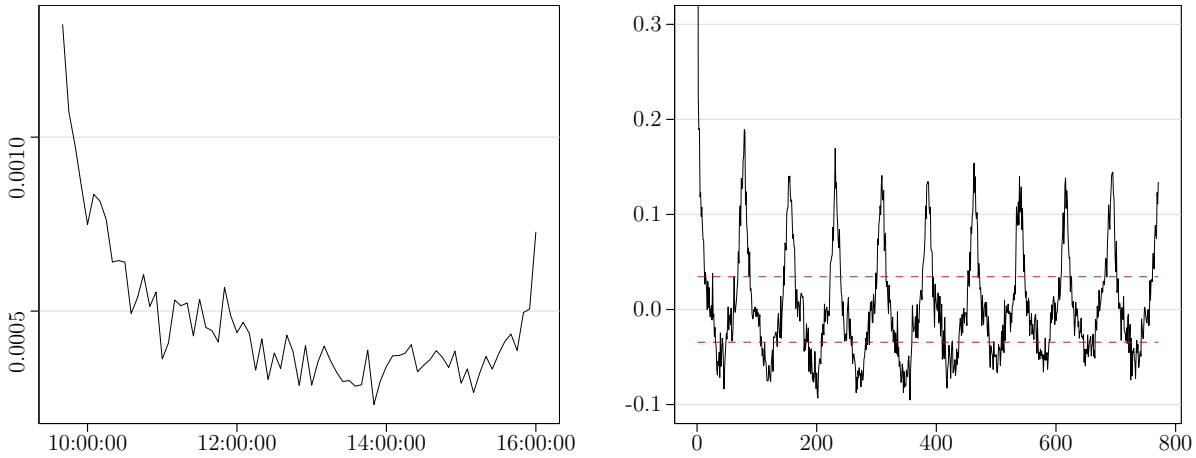

(a) Average absolute 5-minute returns

(b) ACF of absolute 5-minute returns

Figure 1: Daily average and autocorrelation of absolute returns for *JNJ NASDAQ*. *Panel (a) shows the average absolute returns per 5-minute bin over all 42 days, whereas panel (b) presents the autocorrelation function of the exemplary stock JNJ with its corresponding confidence bounds. The other stocks show the same patterns in both of the measures.*

4 Estimating and Filtering the Periodic Component

As mentioned before, we employ a two-step procedure in accordance with Behrendt and Schmidt (2018) to estimate the intraday periodic component. We follow a common approach to decompose the yet unfiltered intraday returns. With the aim to estimate the constituent parts of this specific decomposition described below, we employ an A-PARCH model to calculate the daily volatility factor in the first step, and employ the FFF-Regression and the TX-Estimator method to derive the periodic component in the second step. In the following we provide a more technical explanation of these techniques.

4.1 Return Decomposition Model

We decompose the intraday returns using the general framework proposed by Andersen and Bollerslev (1997) and Andersen and Bollerslev (1998) in the following way

$$\begin{aligned} R_{t,n} &= \mathbb{E}[R_{t,n}] + s_{t,n}\sigma_{t,n}\varepsilon_{t,n}, \\ \varepsilon_{t,n} &\overset{i.i.d.}{\sim} \mathcal{N}(0,1) \end{aligned} \tag{2}$$

where $\sigma_{t,n}$ denotes a 5-minute volatility factor and $s_{t,n}$ the periodic intraday component, which is normalized as in Hecq et al. (2012) so that its squared value is equal to one over the day, i.e.

Assumption 1

$$\frac{1}{N}\sum_{n=1}^{N} s_{t,n}^2 = 1 \quad \forall t$$

Normalization of $s_{t,n}^2$ — Under this model, the standardized returns $(R_{t,n} - \mathbb{E}[R_{t,n}])/\sigma_{t,n}$ are distributed normally with variance $s_{t,n}^2$.

4.2 FFF-Regression (Parametric)

In this section, we describe the parametric FFF-Regression that Andersen and Bollerslev (1997) employ to estimate the periodic intraday component.

By squaring and taking the natural log, Equation 2 can be transformed into a linear regression:

$$\begin{aligned} x_{t,n} &\equiv 2\ln\left(\frac{|R_{t,n} - \mathbb{E}[R_{t,n}]|}{\sigma_{t,n}}\right) \\ &= \ln(s_{t,n}^2) + u_{t,n} \end{aligned} \tag{3}$$

where $u_{t,n}$ is $i.i.d$ with mean zero. As Boudt et al. (2008) note, the estimation of Equation 3 by OLS might not be fully efficient, since $u_{t,n}$ is not normally distributed. However, compared with a maximum likelihood estimator, the loss in efficiency is not dramatic and the OLS estimator is much less sensitive to jumps in the data generating process. Therefore, we choose OLS as an estimation method.

The estimation is a two-step procedure: in the first step, $\mathbb{E}[R_{t,n}]$ is simply estimated by the sample mean, which we denote by $\bar{R}_{t,n}$. For the 5-minute volatility factor we need the assumption of constant intradaily

volatility, i.e.

Assumption 2

$$\sigma_{t,n} = \sqrt{\frac{\sigma_t}{N}}$$

Constant volatility over the day — We obtain an estimate for the daily volatility, σ_t via the A-PARCH model of Ding et al. (1993) using the second dataset of daily returns. The result of the first step is then the estimated value for the left-hand side of Equation 3, i.e.

$$\hat{x}_{t,n} = 2\ln\left(\frac{|R_{t,n} - \bar{R}_{t,n}|}{\hat{\sigma}_{t,n}}\right). \tag{4}$$

In the second step, the log squared periodic component of Equation 3, $\ln(s^2_{t,n})$ is parameterised according to a variant of the Fourier flexible form (Gallant 1981) as given in Andersen and Bollerslev (1997):

$$\begin{aligned}\hat{x}_{t,n} &= \mu_0 + \mu_1\frac{n}{N_1} + \mu_2\frac{n}{N_2} \\ &+ \sum_{p=1}^{P}\gamma_{c,p}\cos\left(\frac{2\pi p}{N}n\right) \\ &+ \gamma_{s,p}\sin\left(\frac{2\pi p}{N}n\right) + \nu_{t,n},\end{aligned} \tag{5}$$

with

$$\begin{aligned}N_1 &= n/((N+1)/2), \\ N_2 &= n/((N+1)(N+1)/6)\end{aligned}$$

which function as normalizing constants. Estimating the right-hand side of this equation by OLS gives us the transformed, unstandardised periodic component (the fitted values), $s^\star_{t,n}$. In order to comply to Assumption 1 we retrieve the estimated periodic component as:

$$\hat{s}_{t,n} = \frac{\exp\left(s^\star_{t,n}\right)}{\sqrt{\frac{1}{N}\sum_{t=1}^{T}\sum_{n=1}^{N}\left[\exp\left(s^\star_{t,n}\right)\right]^2}} \tag{6}$$

where $\hat{s}_{t,n}$ is now standardised so that the daily mean of its square is equivalent to 1 at every day t.

4.3 TX-Estimator (Non-Parametric)

The periodic intraday component can also be estimated in a non-parametric way, as shown by Taylor and Xu (1997) and R. F. Engle and Sokalska (2012).

Here the periodic intraday component is estimated by the variance of the returns in each bin, after deflating them by the daily variance. From Equation 2:

$$\begin{aligned}\frac{(R_{t,n} - \mathbb{E}[R_{t,n}])^2}{\sigma^2_{t,n}} &= s^2_{t,n}\varepsilon^2_{t,n} \\ \mathbb{E}\left[\frac{(R_{t,n} - \mathbb{E}[R_{t,n}])^2}{\sigma^2_{t,n}}\right] &= s^2_{t,n},\end{aligned}$$

assuming that $\mathbb{E}[\varepsilon^2_{t,n}] = 1$. The estimator is then given by the sample equivalent of Equation 7:

$$\hat{s}^2_{t,n} = \frac{1}{T}\sum_{t=1}^{T}\frac{(R_{t,n} - \bar{R}_{t,n})^2}{\hat{\sigma}^2_{t,n}},$$

where we use the definition of the sample mean, the assumption of constant volatility over the day and the daily volatility from the A-PARCH in the same way as above for the FFF-Regression estimator. Finally, we also

normalise this estimate in order to comply to Assumption 1.

4.4 Filtering

Filtering out the periodic component for returns is simply achieved by dividing them by $\hat{s}$. We denote filtered returns as $\widetilde{R}$, i.e.

$$\widetilde{R}_{t,n} = \frac{R_{t,n}}{\hat{s}_{t,n}} \qquad |\widetilde{R}_{t,n}| = \frac{|R_{t,n}|}{\hat{s}_{t,n}}. \qquad (7)$$

5 Filtering Results

In the following we will present the results of our filtering methods. We will only refer to the figures of the filtered returns and their corresponding ACFs for the stock JNJ on the exchange NASDAQ shown in Figure 2 and Figure 3, as all stocks exhibit comparable results. We report the plots for the remaining stocks and exchange in the Appendix in D. The estimated coefficients arising from the A-PARCH model to determine the interdaily volatility component, which are used in both filtering models, can be reviewed in Table 6.

The estimated coefficients from the FFF-Regression described by Equation 5 are reported in Table 5. From the summary table we can see that for most of the stocks our method does not produce many significant estimates – or no significant estimates at all. Although this does not affect the overall significance of our estimated models as can be inferred from the reported F-statistics.

The corresponding fitted values are graphically shown in Figure 4 for the stock exchange NASDAQ. The method models a recurring pattern throughout the full dataset that repeats from day to day. As the dependent variable here is the log squared standardised return, it is somewhat difficult to observe the pattern fit. However, the fit of the final result of the FFF-estimation, as shown in Figure 2a, signifies that the FFF-Regression can achieve a decent fit to the U-shape in the average absolute 5-minute returns. The resulting *filtered* absolute 5-minute returns seem to be stationary judged by the eye alone.

Since the TX-Estimator is non-parametric, there are no estimation results to report, but only the fit of the estimated periodic component as in Figure 3. Compared to the FFF-Regression it is much more noisy and resembles the shape of the average absolute 5-minute returns, which indicates that it fits the data more closely. The resulting filtered average absolute 5-minute returns also clearly show less volatility than those of the FFF-Regression results.

As we plan to forecast the volatility with the filtered returns utilizing a GARCH(1,1) model, prerequisites like the stationarity of the return series and an exponentially declining autocorrelation function are required. In order to confirm the stationarity requirement, we conduct augmented Dickey-Fuller Tests (hereinafter ADF tests) and report the results in Table 2 for the FFF-Regression and in Table 3 for the TX-Estimation method respectively.

The ADF tests include both a constant

Table 2: FFF – ADF test results

Ticker	DF statistic	p-value
NASDAQ		
JNJ	-15.51789	0.01
JPM	-14.46741	0.01
PG	-13.95715	0.01
T	-14.09849	0.01
WFC	-15.25767	0.01
WMT	-15.11362	0.01
XOM	-15.67289	0.01
NYSE		
JNJ	-15.32871	0.01
JPM	-14.45121	0.01
PG	-13.96439	0.01
T	-14.06793	0.01
WFC	-15.19751	0.01
WMT	-15.14850	0.01
XOM	-15.61136	0.01

Table 3: TX – ADF test results

Ticker	DF statistic	p-value
NASDAQ		
JNJ	-15.60358	0.01
JPM	-14.45235	0.01
PG	-14.14905	0.01
T	-14.02696	0.01
WFC	-14.97904	0.01
WMT	-15.15984	0.01
XOM	-15.77055	0.01
NYSE		
JNJ	-15.53992	0.01
JPM	-14.46406	0.01
PG	-14.13650	0.01
T	-14.01555	0.01
WFC	-14.96331	0.01
WMT	-15.15831	0.01
XOM	-15.75455	0.01

and a linear trend. For all the filtered returns series we can reject the null hypothesis of having a unit root on the 1% significance level. Thus, we can conclude, that the filtered returns series are stationary and therefore suited for our further undertaking.

A second, more crucial criterion which we already addressed in previous sections, is that of an exponentially declining shape in the autocorrelation function. This is to our understanding equally achieved by both of the filtering methods, reported in Figure 2b and Figure 3b. Though the wavelike pattern is not completely eliminated and still persists to some extent, we can argue that this is negligible since we do not observe too many significant values.

6 Forecasting Model

After accounting for the intraday periodicity through the filtering process, we model the remaining intraday dynamics with a GARCH(1,1) model, which is common in the literature and a sufficient model in most cases. Following R. F. Engle and Sokalska (2012), we first deflate the returns by the daily volatility and the intraday periodic volatility

$$z_{t,n} = \frac{R_{t,n} - \bar{R}_{t,n}}{\hat{\sigma}_{t,n}\hat{s}_{t,n}},$$

giving us the residual volatility. The GARCH(1,1) specification is then defined

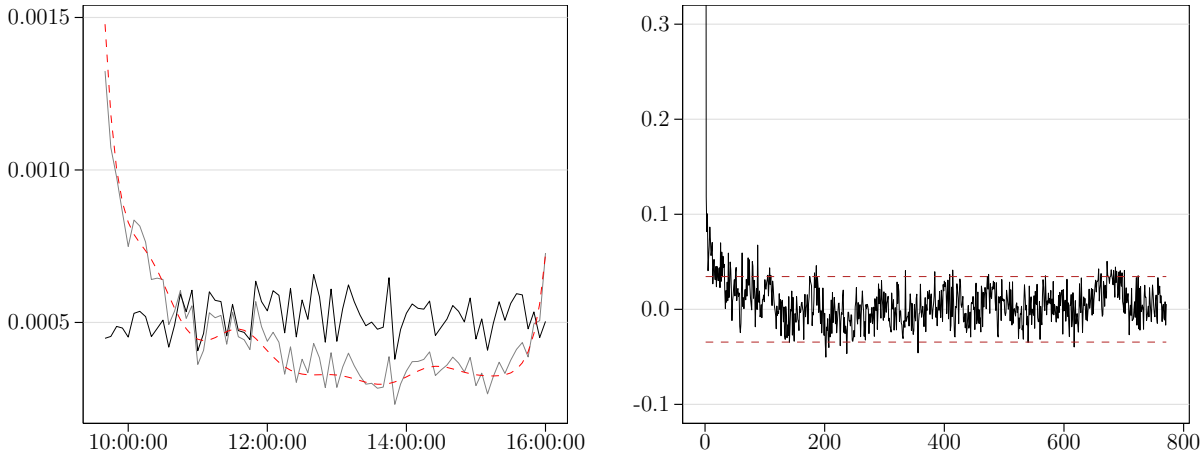

(a) Filtered returns series

(b) ACF of filtered returns

Figure 2: Filtered daily average and autocorrelation of absolute returns for *JNJ NASDAQ*. *Panel (a) shows the average absolute returns per 5-minute bin over all 42 days (gray solid line) as well as the FFF estimate for the periodic intraday component (red dashed line) and the filtered returns (black solid line), whereas panel (b) presents the autocorrelation function of the exemplary stock with its corresponding confidence bounds.*

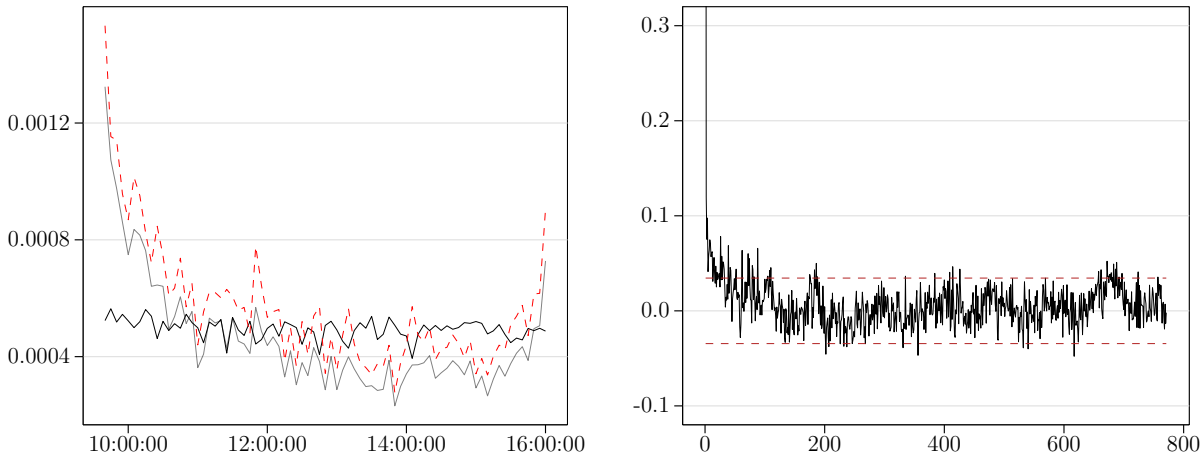

(a) Filtered returns series

(b) ACF of filtered returns

Figure 3: Filtered daily average and autocorrelation of absolute returns for *JNJ NASDAQ*. *Panel (a) shows the average absolute returns per 5-minute bin over all 42 days (gray solid line) as well as the TX-Estimate for the periodic intraday component (red dashed line) and the filtered returns (black solid line), whereas panel (b) presents the autocorrelation function of the exemplary stock with its corresponding confidence bounds.*

as follows:

$$z_{t,n}|F_{t,n-1} \sim \mathcal{N}(0, q_{t,n})$$
$$q_{t,n} = \omega + \alpha z_{t,n-1}^2 + \beta q_{t,n-1}.$$

After applying the common measures and tests, we can confirm the convergence of the above specified GARCH-model for all observed stocks and exchanges.

For the purpose of forecasting, we split up the sample into a training set, containing the first 80% of observations, and a testing set with the remaining 20% of observations. The forecasts $\tilde{q}_{t,n}$ are then derived via one-step-ahead forecasting. This mimics the approach a trader would employ in practice, where the whole set of information up to the present point in time is used to get the best prediction for the next point in time.

6.1 Forecasting Results

We compare the forecasting performance of the FFF versus the TX-Estimation method with the same approach as R. F. Engle and Sokalska (2012). As they state, we forecast a variable that cannot be observed and therefore need a proxy for, which will be represented by the squared return $z_{t,n}^2 = R_{t,n}^2/(\hat{\sigma}_{t,n}^2 \hat{s}_{t,n}^2)$. Combined with the two performance measures based on the mean squared error and the out-of-sample likelihood,

$$MSE = \frac{1}{TN} \sum_{n=0.8N}^{N} \sum_{t=0.8T}^{T} (z_{t,n}^2 - \tilde{q}_{t,n}^2)^2$$
$$LIK = \frac{1}{TN} \sum_{n=0.8N}^{N} \sum_{t=0.8T}^{T} \left(\ln(\tilde{q}_{t,n}^2) + \frac{z_{t,n}^2}{\tilde{q}_{t,n}^2} \right)$$

optimal forecasts based on the squared filtered return $z_{t,n}^2$ are unbiased.

We report the forecast performance results in Table 4. As can easily be seen, the forecasts based on the TX-Estimator outclasses the FFF-Regression method in almost all cases.

Regarding the very small differences in the MSE performance measure between our two filtering approaches and across all stocks however, we cannot conclude for an exact norm that inevitably favors filtering via the TX-Method. On the other hand indeed, the LIK performance measure hints towards the TX-Method more clearly.

Interestingly, the only ticker for which the forecasting results deliver no unambiguous inference as to whether the FFF or TX-Method is to be favored based on the selected performance measures, happens to refer to the stock (PG) that produced the most significant estimated in our FFF-Regression. This circumstance however could hint towards a possible misspecification in the aforementioned model. In order to address these concerns we tested our analysis for different tuning parameters P in the FFF-Regression. Although we find some changes in the significance of several estimates, the overall conclusion on the forecasting performance

	MSE		LIK	
Ticker	FFF	TX	FFF	TX
NASDAQ				
JNJ	0.0003595	**0.0003595**	-3.7	**-3.83**
JPM	0.0001558	**0.0001558**	-4.08	**-4.14**
PG	0.0001619	**0.0001619**	**-4.04**	-3.97
T	0.0003147	**0.0003147**	-3.99	**-4.02**
WFC	0.0001491	**0.0001491**	-4.1	**-4.19**
WMT	0.0001139	**0.0001139**	-4.13	**-4.28**
XOM	0.001637	**0.001637**	-3.28	**-3.46**
NYSE				
JNJ	0.0003668	**0.0003668**	-3.72	**-3.81**
JPM	0.0001493	**0.0001493**	-4.09	**-4.13**
PG	0.0001615	**0.0001615**	**-4.05**	-3.99
T	0.0003068	**0.0003068**	-3.99	**-4.02**
WFC	0.0001423	**0.0001423**	-4.11	**-4.19**
WMT	0.0001126	**0.0001126**	-4.13	**-4.27**
XOM	0.0017427	**0.0017427**	-3.27	**-3.46**

Table 4: *Results for the MSE and LIK forecast performance measures for the forecasts based on both the FFF-Regression and the TX-Estimator. Values in* ***bold*** *indicate the superior measure.*

as in Table 4 is not affected. Therefore we again follow Behrendt and Schmidt (2018, p. 366) and remain with a tuning parameter of $P = 6$, as this happens to be standard in the common literature.

7 Discussion and Conclusion

In this paper we employed two different approaches to estimate and filter the periodic, U-shaped pattern that is common in intraday stock and foreign exchange return volatility, in order to optimise intraday volatility forecasts. The analysed dataset consists of 1-second returns of 7 stocks and covers the exchanges NYSE and NASDAQ. In order to mitigate the noise common in high-frequency data, we aggregated the returns to the 5-minute frequency. Both approaches are based on a decomposition of these returns into multiplicative components, namely the periodic pattern, a 5-minute volatility factor and an idiosyncratic error.

The 5-minute volatility factor was derived via an A-PARCH model of daily returns for all stocks, covering the period from 2010 to 2017. The resulting daily volatility estimates were divided by the number of daily 5-minute returns to to derive the volatility factor. This of course means that this volatility is constant over the day, an assumption that could be relaxed in order to get a more realistic model. However, since the focus of this paper lies on forecasting, and the assumption is equal over both es-

timation and filtering approaches, we employed this more simple model.

The first approach is based on a Fourier flexible form parametrisation, called FFF-Regression. This method uses trigonometric functions to model the repeating pattern. Although our fitted regression estimates are jointly significant for each individual stock, we do not find the individual parameters to be significant, except for two stocks. Contrary to results from other papers, including more or excluding trigonometric terms in the regression model does not change this situation. This could be due to the fact that our model assumes that the pattern is equal for each individual day. As it is known that there are also differences in return volatility depending on the day of week (see e.g. Harris (1986)), relaxing this assumption might yield better results. However, we are limited in the approach to estimate the pattern separately for each weekday, since our sample only covers the period of two months. Also, since comparable studies (e.g. Behrendt and Schmidt (2018)) cover much longer time periods, the simple model could suffice given enough data. But even with these limited results, the filtered returns based on this approach are stationary and show exponentially declining autocorrelations, meaning that forecasts based on GARCH-models can be conducted.

The second approach is based on a non-parametric estimator, which uses the sample variance for all returns in an intraday "bin", which we call TX-Estimator. As there is no model estimation involved, judgment of the quality of this estimator is based on the quality of the resulting forecasts. Graphically we observe that this estimator is much more noisy compared to the FFF-Regression, and fits the U-shaped pattern much more closely. The filtered returns from this approach also show the desired properties of stationarity and exponentially declining autocorrelations.

After filtering the periodic component out of the returns, we employ standard GARCH(1,1) models to estimate and forecast the intraday volatility. The forecasts are one-step-ahead forecasts and are compared to the squared returns via two loss functions, based on the mean squared error and the out-of-sample likelihood. Although the differences are very small, the TX-Estimator performs better in almost all cases for both metrics. The only case in which the FFF-Regression based forecast performs better, is the one where it produced significant parameter estimates. Based on our data sample, our findings would support the view that the TX-Estimator performs better. However since this sample is quite small, the FFF-Regression might not be a feasible approach here and a larger sample might yield the result that it performs superior to the TX-Estimator.

References

Admati, Anat R. and Paul Pfleiderer (Jan. 1988). "A Theory of Intraday Patterns: Volume and Price Variability". In: *Review of Financial Studies* 1.1, pp. 3–40. DOI: 10.1093/rfs/1.1.3.

Alexander, Carol (2008). *Market risk analysis*. Chichester, England ; Hoboken, NJ: Wiley.

Andersen, Torben G. and Tim Bollerslev (June 1997). "Intraday periodicity and volatility persistence in financial markets". In: *Journal of Empirical Finance* 4.2, pp. 115–158. DOI: 10.1016/S0927-5398(97)00004-2.

– (Feb. 1998). "Deutsche Mark-Dollar Volatility: Intraday Activity Patterns, Macroeconomic Announcements, and Longer Run Dependencies". In: *The Journal of Finance* 53.1, pp. 219–265. DOI: 10.1111/0022-1082.85732.

Baillie, Richard T. and Tim Bollerslev (May 1, 1991). "Intra-Day and Inter-Market Volatility in Foreign Exchange Rates". In: *The Review of Economic Studies* 58.3, pp. 565–585. DOI: 10.2307/2298012.

Behrendt, Simon and Alexander Schmidt (Nov. 2018). "The Twitter myth revisited: Intraday investor sentiment, Twitter activity and individual-level stock return volatility". In: *Journal of Banking & Finance* 96, pp. 355–367. DOI: 10.1016/j.jbankfin.2018.09.016.

Black, Fischer and Myron Scholes (May 1973). "The Pricing of Options and Corporate Liabilities". In: *Journal of Political Economy* 81.3, pp. 637–654. DOI: 10.1086/260062.

Bollerslev, Tim and Ian Domowitz (1993). "Trading Patterns and Prices in the Interbank Foreign Exchange Market". In: *The Journal of Finance* 48.4, pp. 1421–1443. DOI: 10.1111/j.1540-6261.1993.tb04760.x.

Boudt, Kris et al. (2008). "Robust Estimation of Intraweek Periodicity in Volatility and Jump Detection". In: *Journal of Empirical Finance* 18, pp. 353–367. DOI: 10.2139/ssrn.1297371.

Brownlees, C.T. and G.M. Gallo (Dec. 2006). "Financial econometric analysis at ultra-high frequency: Data handling concerns". In: *Computational Statistics & Data Analysis* 51.4, pp. 2232–2245. DOI: 10.1016/j.csda.2006.09.030.

Dacorogna, Michael M. et al. (Aug. 1, 1993). "A geographical model for the daily and weekly seasonal volatility in the foreign exchange market". In: *Journal of International Money and Finance* 12.4, pp. 413–438. DOI: 10.1016/0261-5606(93)90004-U.

Ding, Zhuanxin et al. (June 1993). "A long memory property of stock market returns and a new model". In: *Journal of Empirical Finance* 1.1, pp. 83–106. DOI: 10.1016/0927-5398(93)90006-D.

Engle, R. F. and M. E. Sokalska (Jan. 1, 2012). "Forecasting intraday volatility in the US equity market. Multiplicative component GARCH". In: *Journal of Financial Econometrics* 10.1, pp. 54–83. DOI: 10.1093/jjfinec/nbr005.

Engle, Robert F. (2000). "The Econometrics of Ultra-high-frequency Data". In: *Econometrica* 68.1, pp. 1–22. DOI: 10.1111/1468-0262.00091.

Fama, Eugene F and Kenneth R French (2004). "The Capital Asset Pricing Model: Theory and Evidence". In: *Journal of Economic Perspectives* 18.3, pp. 25–46. DOI: 10.1257/0895330042162430.

Gallant, A. Ronald (1981). "On the bias in flexible functional forms and an essentially unbiased form: the Fourier flexible form". In: *Journal of Econometrics* 15.2, pp. 211–245. DOI: 10.1016/0304-4076(81)90115-9.

Hansen, Peter R and Asger Lunde (Apr. 2006). "Realized Variance and Market Microstructure Noise". In: *Journal of Business & Economic Statistics* 24.2, pp. 127–161. DOI: 10.1198/073500106000000071.

Harris, Lawrence (May 1, 1986). "A transaction data study of weekly and intradaily patterns in stock returns". In: *Journal of Financial Economics* 16.1, pp. 99–117. DOI: 10.1016/0304-405X(86)90044-9.

Hecq, A. et al. (Apr. 1, 2012). "Common Intraday Periodicity". In: *Journal of Financial Econometrics* 10.2, pp. 325–353. DOI: 10.1093/jjfinec/nbr012.

Jain, Prem C. and Gun-Ho Joh (Sept. 1988). "The Dependence between Hourly Prices and Trading Volume". In: *Journal of Financial and Quantitative Analysis* 23.3, pp. 269–283. DOI: 10.2307/2331067.

Müller, Ulrich A. et al. (Dec. 1, 1990). "Statistical study of foreign exchange rates, empirical evidence of a price change scaling law, and intraday analysis". In: *Journal of Banking & Finance* 14.6, pp. 1189–1208. DOI: 10.1016/0378-4266(90)90009-Q.

Poon, Ser-Huang and Clive W. J Granger (June 2003). "Forecasting Volatility in Financial Markets: A Review". In: *Journal of Economic Literature* 41.2, pp. 478–539. DOI: 10.1257/002205103765762743.

Taylor, Stephen J. and Xinzhong Xu (Dec. 1, 1997). "The incremental volatility information in one million foreign exchange quotations". In: *Journal of Empirical Finance* 4.4. DOI: 10.1016/S0927-5398(97)00010-8.

Wood, Robert A. et al. (1985). "An Investigation of Transactions Data for NYSE Stocks". In: *The Journal of Finance* 40.3, pp. 723–739. DOI: 10.1111/j.1540-6261.1985.tb04996.x.

Zhou, Bin (Jan. 1996). "High-Frequency Data and Volatility in Foreign-Exchange Rates". In: *Journal of Business & Economic Statistics* 14.1, pp. 45–52. DOI: 10.1080/07350015.1996.10524628.

A FFF-Regression

A.1 OLS Estimation Summary

Table 5: FFF-Regression Estimation Results

(a) NASDAQ

	JNJ	JPM	PG	T	WFC	WMT	XOM
norm1	−24.56**	−13.33	−38.39***	−16.14	−4.08	−6.80	−15.61
norm2	8.05*	4.15	12.73***	5.24	1.06	2.03	5.11
cos1	−4.10*	−1.99	−6.91***	−2.38	−0.13	−0.56	−2.41
cos2	−0.98*	−0.53	−1.61***	−0.77	0.02	−0.11	−0.46
cos3	−0.30	−0.18	−0.66**	0.08	0.01	0.20	−0.20
cos4	−0.16	−0.16	−0.34**	−0.16	0.09	0.07	−0.05
cos5	−0.12	−0.16	−0.35***	−0.12	0.02	0.08	0.05
cos6	−0.02	−0.12	−0.22**	0.02	0.002	0.01	−0.10
sin1	−0.12	−0.35	−0.22	0.14	0.005	0.08	0.34
sin2	−0.06	0.08	−0.21*	0.10	0.12	0.12	0.16
sin3	0.09	0.03	−0.06	−0.08	−0.02	0.07	0.04
sin4	0.08	−0.03	−0.16*	0.02	0.03	−0.003	0.09
sin5	−0.08	−0.17	−0.06	−0.04	−0.07	0.03	−0.20*
sin6	−0.02	−0.11	−0.01	−0.03	0.10	0.20*	0.26**
Constant	6.69*	2.60	11.02***	2.80	−0.66	0.26	2.83
F Statistic	18.61***	8.77***	16.57***	13.58***	10.01***	17.93***	15.78***

(b) NYSE

	JNJ	JPM	PG	T	WFC	WMT	XOM
norm1	−28.50**	−6.90	−41.58***	−18.61	3.15	−6.55	−21.34
norm2	9.41**	2.00	13.80***	6.02	−1.44	1.95	7.01
cos1	−4.96**	−0.73	−7.53***	−2.84	1.32	−0.49	−3.51
cos2	−1.18**	−0.21	−1.74***	−0.88	0.36	−0.07	−0.73
cos3	−0.38	0.02	−0.74***	0.03	0.18	0.18	−0.32
cos4	−0.21	−0.08	−0.37**	−0.18	0.19	0.08	−0.09
cos5	−0.12	−0.10	−0.35***	−0.14	0.06	0.09	0.03
cos6	−0.08	−0.09	−0.24**	0.01	0.02	0.04	−0.13
sin1	−0.07	−0.24	−0.26	0.002	−0.08	0.08	0.21
sin2	−0.07	0.08	−0.24*	0.04	0.07	0.11	0.13
sin3	0.08	0.04	−0.07	−0.13	−0.06	0.08	−0.01
sin4	0.07	0.02	−0.18*	−0.02	0.05	−0.05	0.08
sin5	−0.02	−0.19*	−0.07	−0.06	−0.08	0.04	−0.26**
sin6	−0.02	−0.05	−0.01	−0.06	0.09	0.20*	0.24**
Constant	7.98**	0.42	12.09***	3.71	−2.96	0.13	4.82
F Statistic	18.52***	9.38***	16.36***	12.76***	9.82***	16.71***	15.97***

*p < .05; **p < .01; ***p < .001

A.2 FFF-Regression Fits

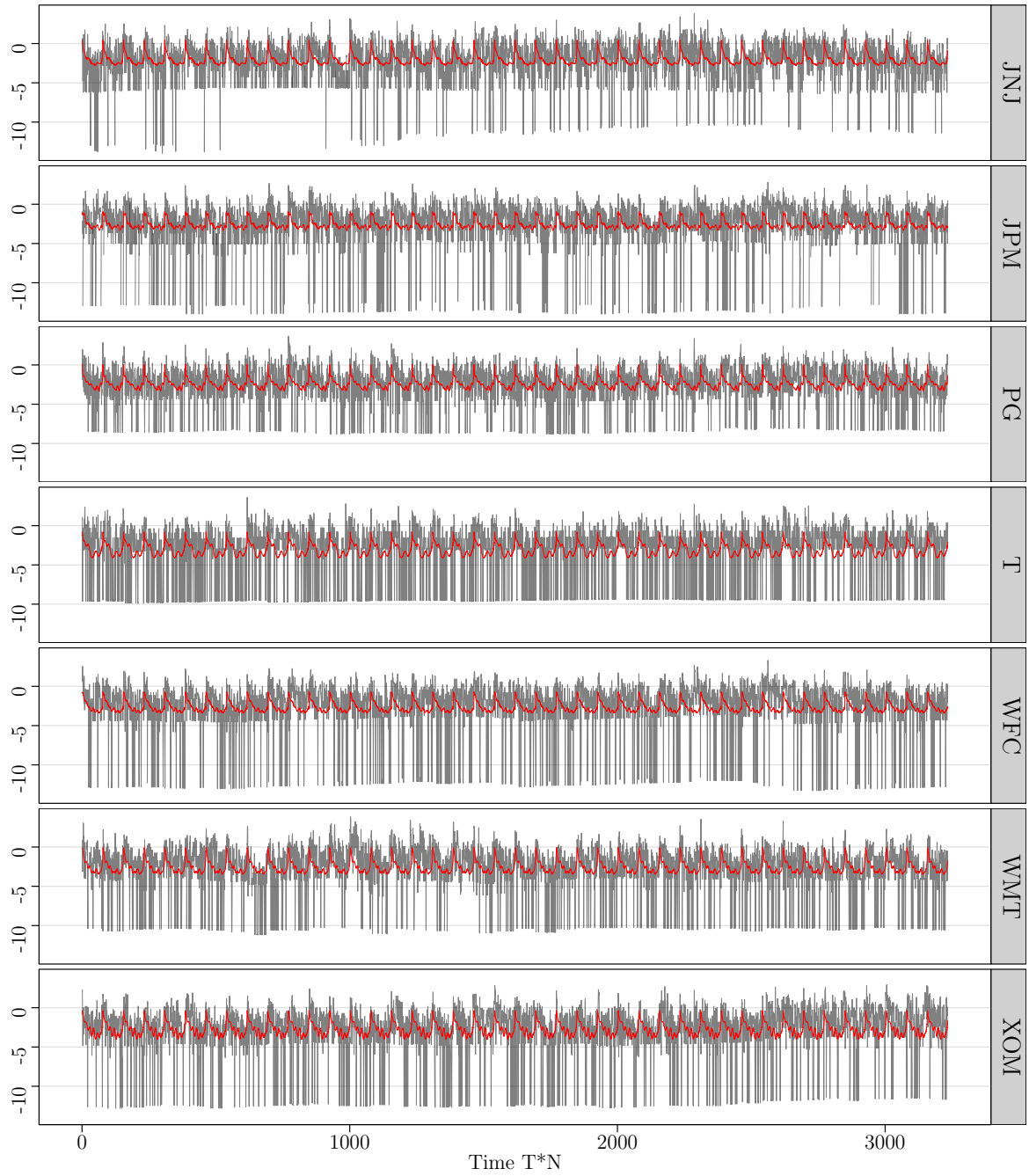

Figure 4: FFF Regression fits for all stocks of the NASDAQ exchange. The estimated periodic component $s^{\star}_{t,n}$ is depicted in red, the log squared standardized returns $\hat{x}_{t,n}$ in black.

B A-PARCH Summary

Table 6: A-PARCH Estimation Results

	JNJ	JPM	PG	T	WFC	WMT	XOM
mu	0.0004*	0.0003	0.0004***	0.0001	0.0002	0.0004	−0.00
omega	0.0002***	0.001***	0.02***	0.0003*	0.0003***	0.003***	0.004***
alpha1	0.10***	0.08***	0.07***	0.05**	0.11***	0.24***	0.09***
gamma1	0.50***	0.83***	0.68***	0.35	0.50***	0.34**	0.57***
beta1	0.85***	0.91***	0.89***	0.87***	0.88***	0.11	0.90***
delta	1.26***	0.77***	0.18	1.26***	1.08***	1.18**	0.48**
Log Likelihood	-6,781.04	2,866.22	3,051.15	-6,392.50	-5,348.83	-6,387.33	2,921.28
AIC	-6.73	2.86	3.04	-6.35	-5.31	-6.34	2.91
BIC	-6.72	2.87	3.06	-6.33	-5.29	-6.33	2.93

*p < .05; **p < .01; ***p < .001

C Average absolute Returns and ACF Functions

Figure 5: Daily average and autocorrelation of absolute returns for *JNJ NYSE*

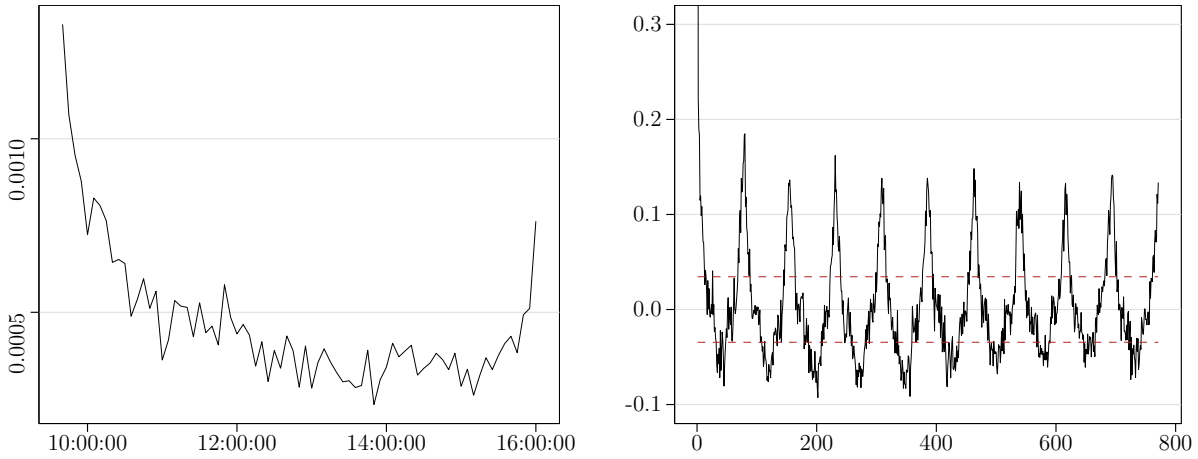

(a) Average absolute 5-minute returns

(b) ACF of absolute 5-minute returns

Figure 6: Daily average and autocorrelation of absolute returns for *JPM NASDAQ*

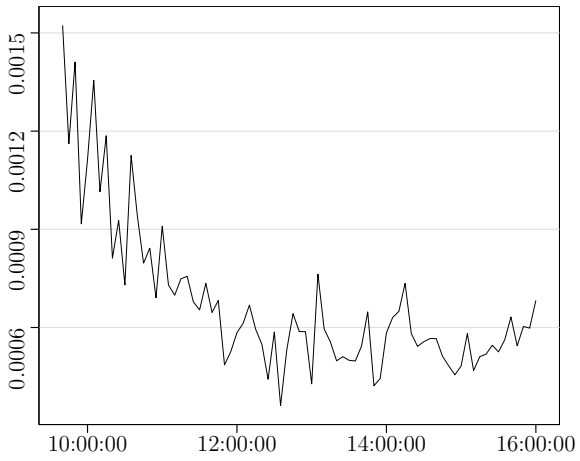

(a) Average absolute 5-minute returns

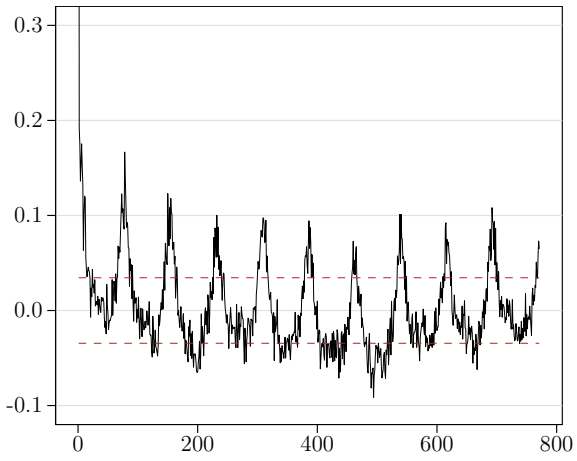

(b) ACF of absolute 5-minute returns

Figure 7: Daily average and autocorrelation of absolute returns for *JPM NYSE*

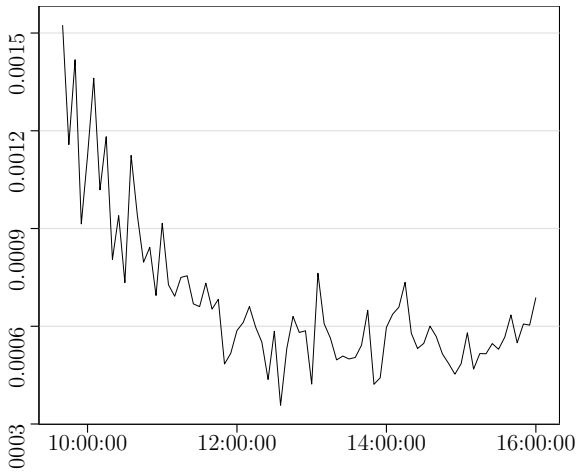

(a) *Average absolute returns per intraday 5-minute "bin" over all 42 days.*

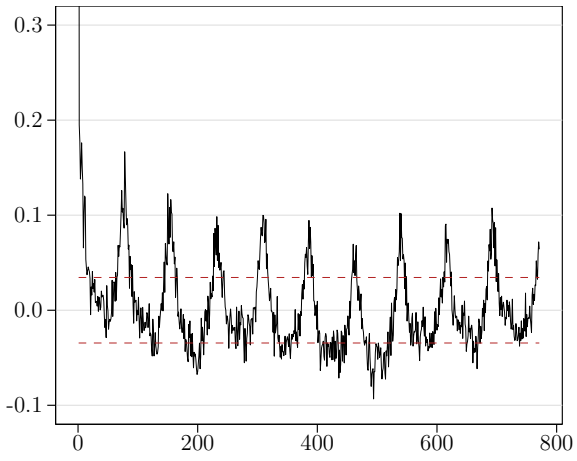

(b) ACF of absolute 5-minute returns

Figure 8: Daily average and autocorrelation of absolute returns for *PG NASDAQ*

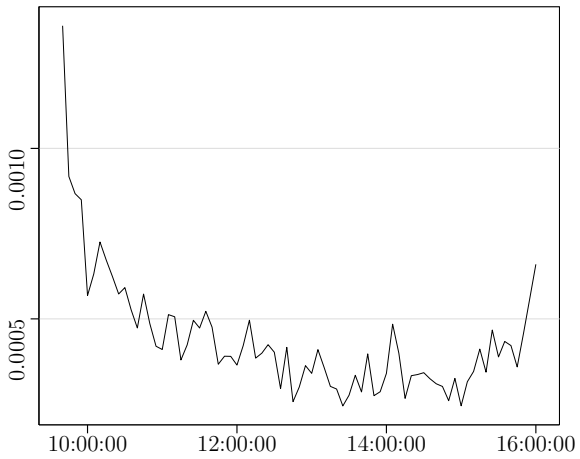

(a) Average absolute 5-minute returns

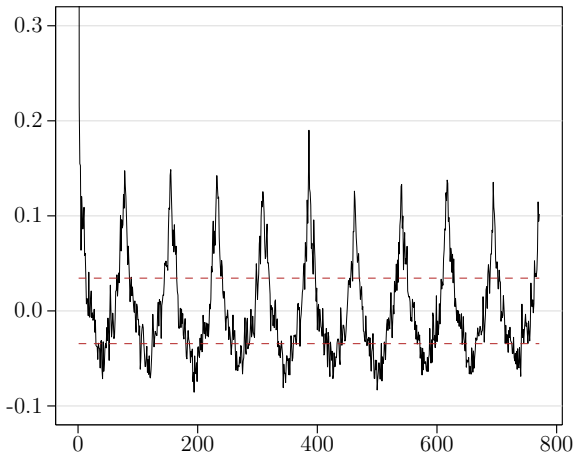

(b) ACF of absolute 5-minute returns

Figure 9: Daily average and autocorrelation of absolute returns for *PG NYSE*

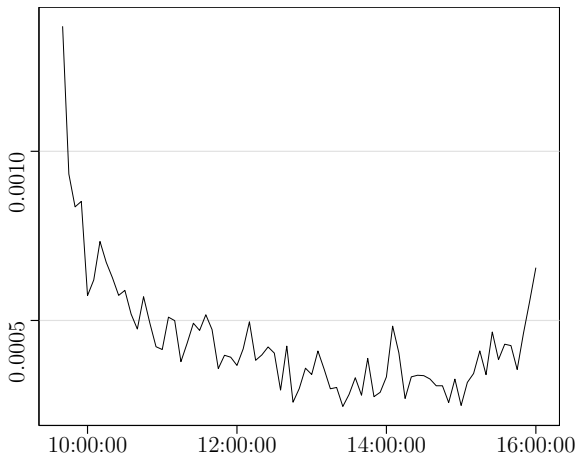

(a) Average absolute 5-minute returns

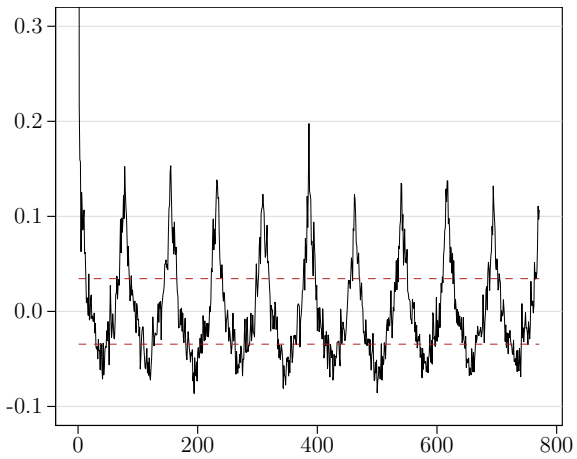

(b) ACF of absolute 5-minute returns

Figure 10: Daily average and autocorrelation of absolute returns for *T NASDAQ*

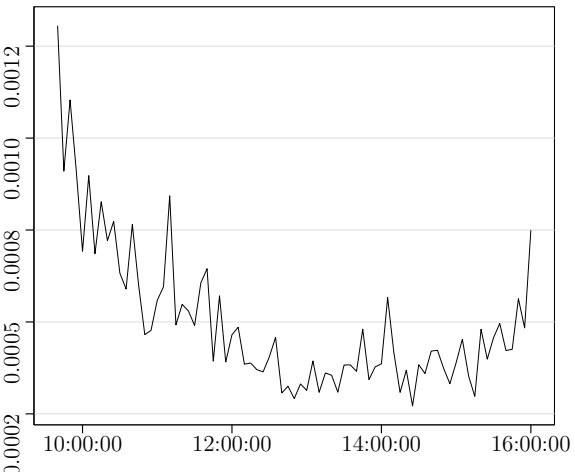

(a) Average absolute 5-minute returns

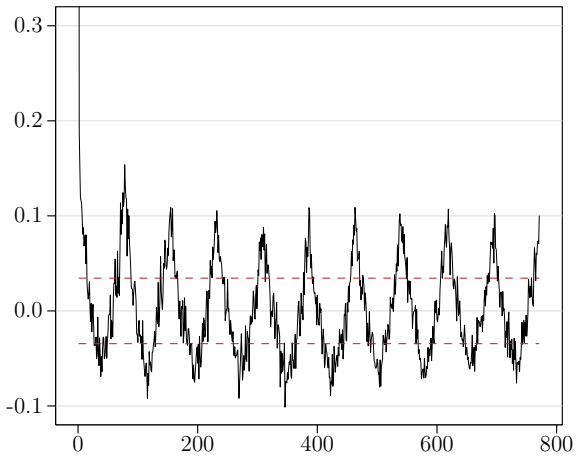

(b) ACF of absolute 5-minute returns

Figure 11: Daily average and autocorrelation of absolute returns for *T NYSE*

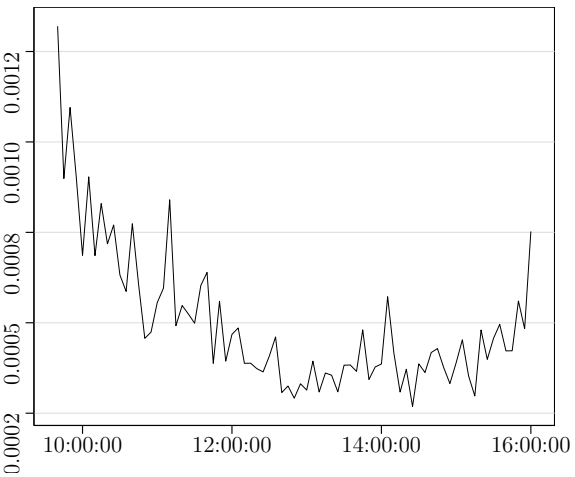

(a) Average absolute 5-minute returns

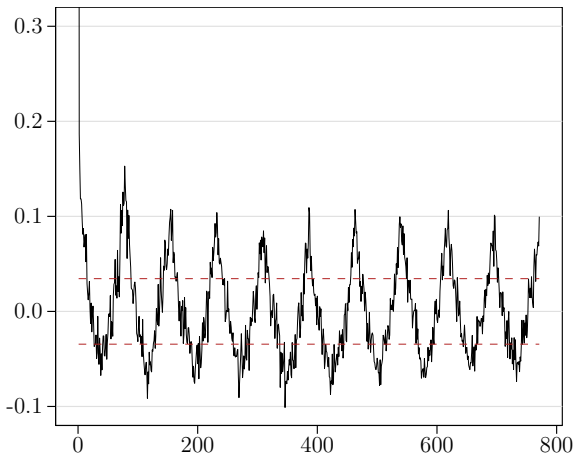

(b) ACF of absolute 5-minute returns

Figure 12: Daily average and autocorrelation of absolute returns for *WFC NASDAQ*

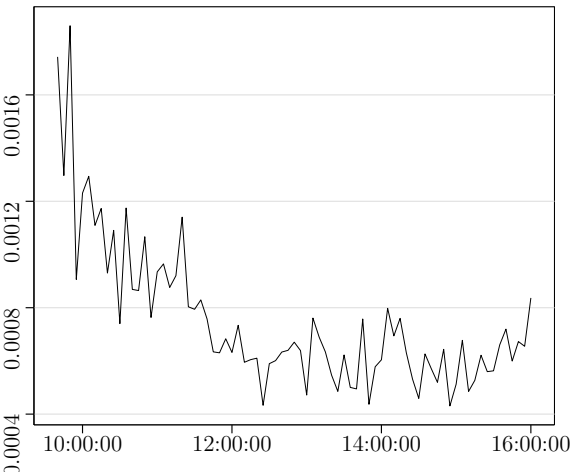

(a) Average absolute 5-minute returns

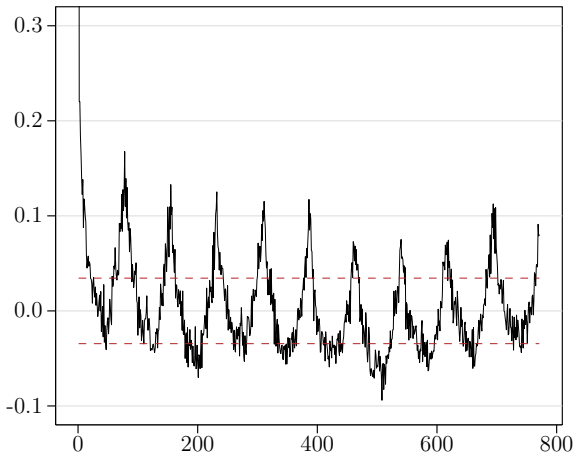

(b) ACF of absolute 5-minute returns

Figure 13: Daily average and autocorrelation of absolute returns for *WFC NYSE*

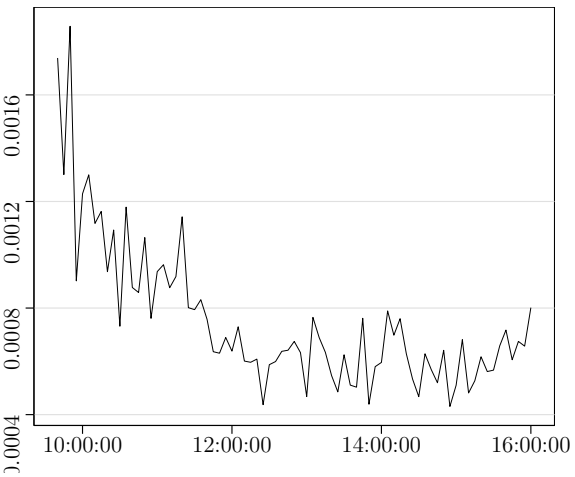

(a) Average absolute 5-minute returns

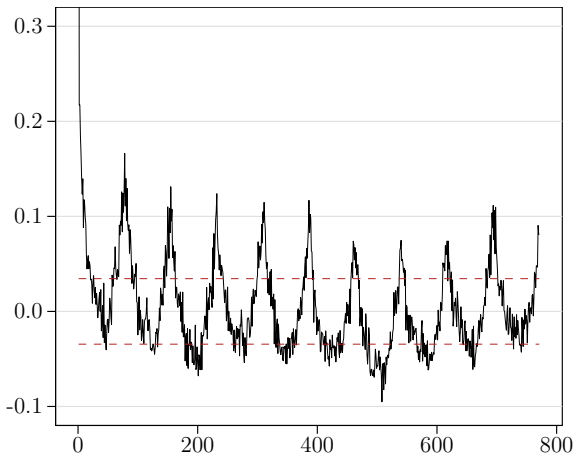

(b) ACF of absolute 5-minute returns

Figure 14: Daily average and autocorrelation of absolute returns for *WMT NASDAQ*

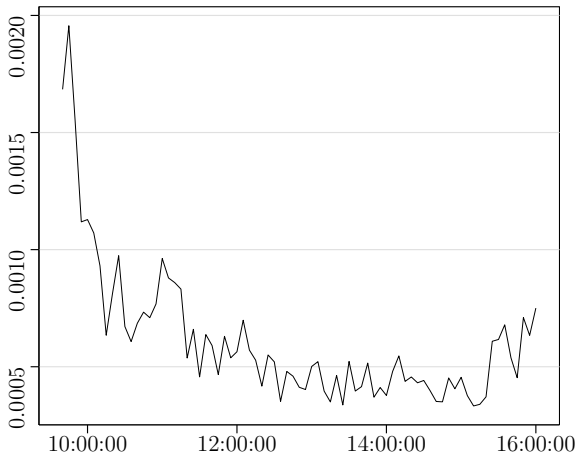

(a) Average absolute 5-minute returns

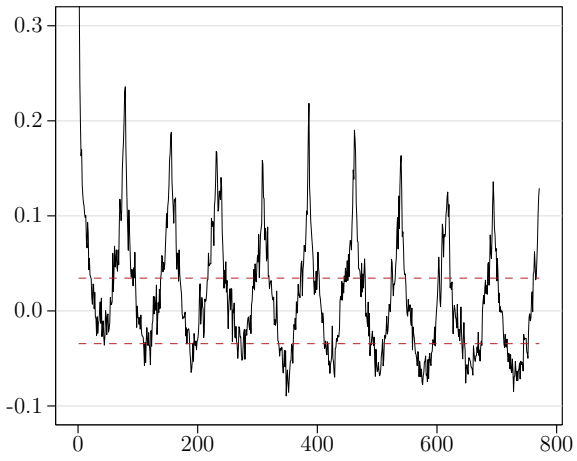

(b) ACF of absolute 5-minute returns

Figure 15: Daily average and autocorrelation of absolute returns for *WMT NYSE*

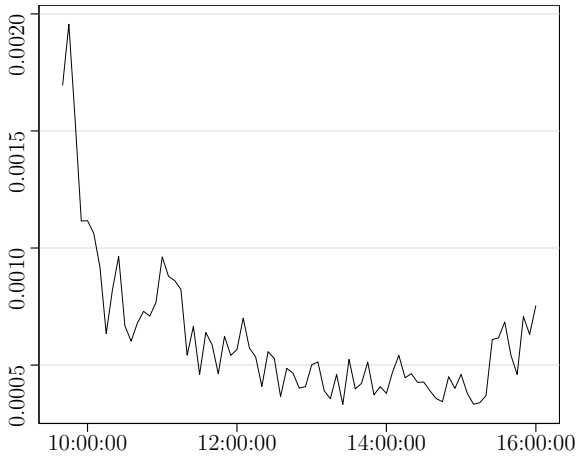

(a) Average absolute 5-minute returns

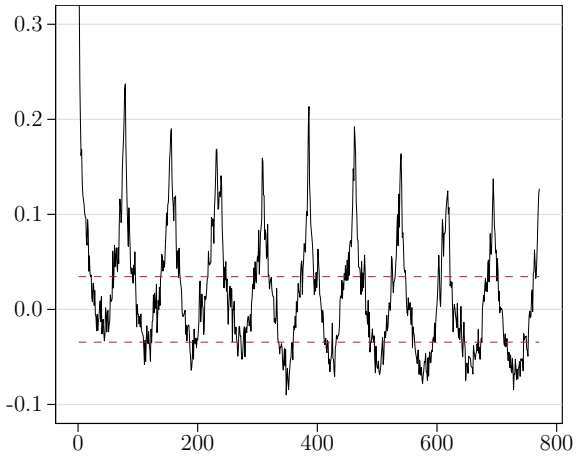

(b) ACF of absolute 5-minute returns

Figure 16: Daily average and autocorrelation of absolute returns for *XOM NASDAQ*

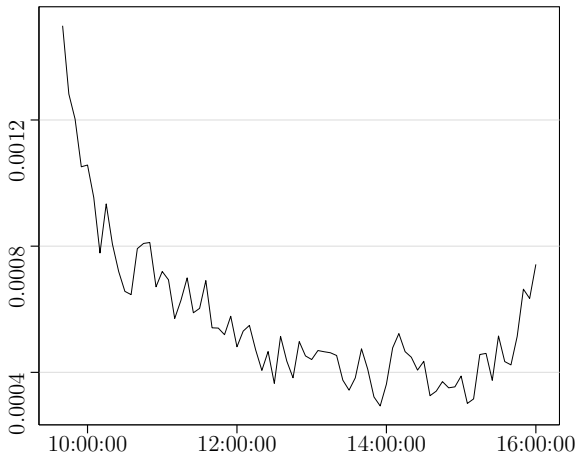

(a) Average absolute 5-minute returns

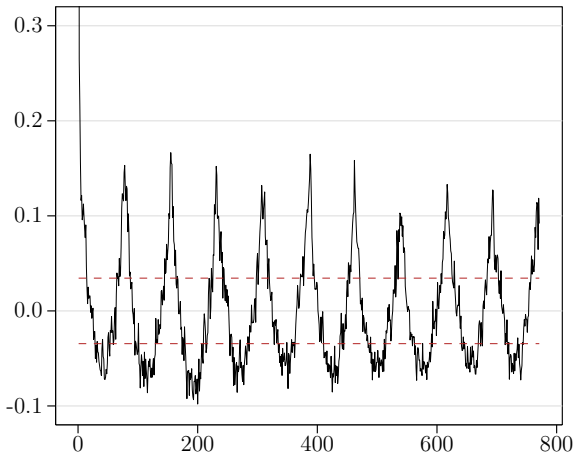

(b) ACF of absolute 5-minute returns

Figure 17: Daily average and autocorrelation of absolute returns for *XOM NYSE*

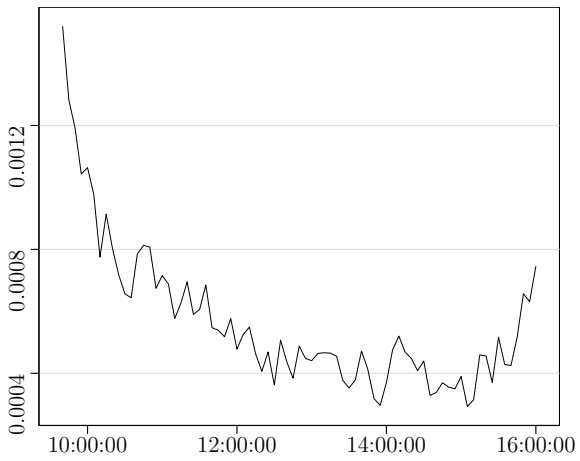

(a) Average absolute 5-minute returns

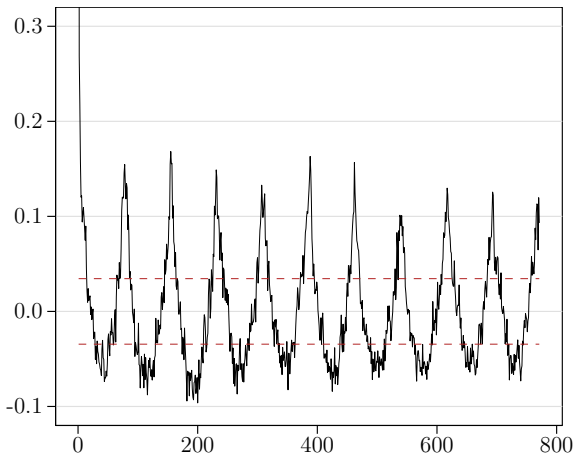

(b) ACF of absolute 5-minute returns

D Filtered average absolute Returns and ACF Functions

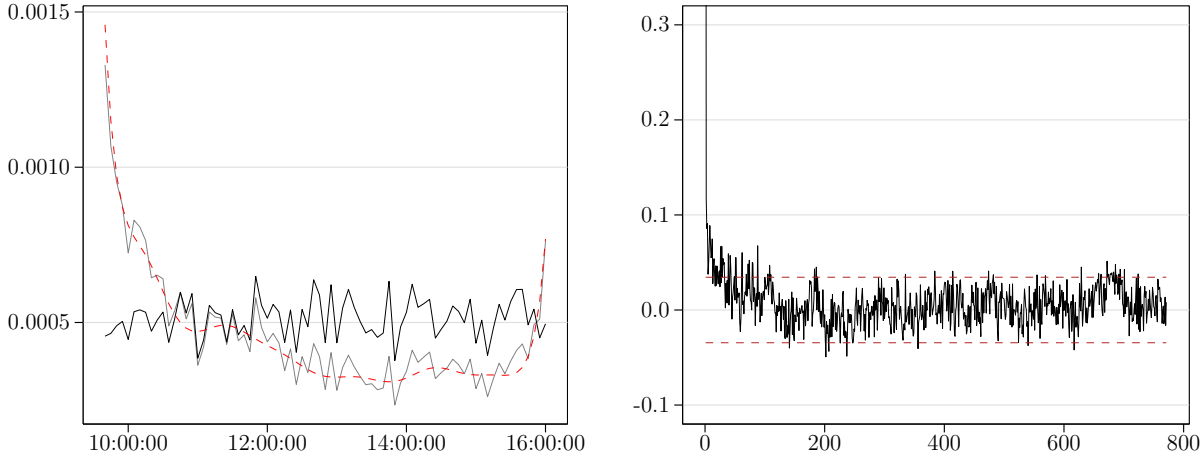

(a) Filtered returns series (b) ACF of filtered returns

Figure 18: Filtered daily average and autocorrelation of absolute returns for *JNJ NYSE*. *Panel (a) shows the average absolute returns per 5-minute bin over all 42 days (gray solid line) as well as the FFF estimate for the periodic intraday component (red dashed line) and the filtered returns (black solid line), whereas panel (b) presents the autocorrelation function of the exemplary stock with its corresponding confidence bounds.*

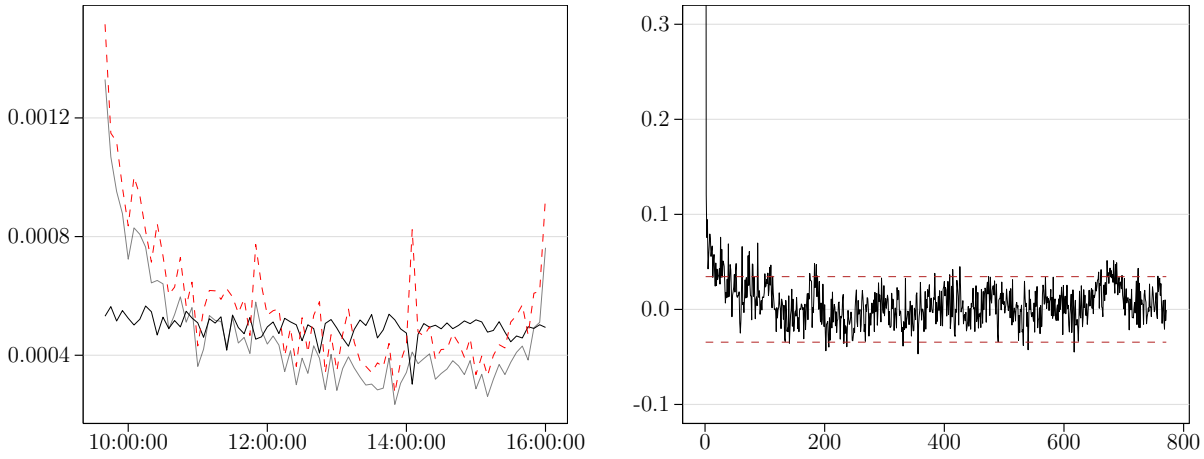

(a) Filtered returns series (b) ACF of filtered returns

Figure 19: Filtered daily average and autocorrelation of absolute returns for *JNJ NYSE*. *Panel (a) shows the average absolute returns per 5-minute bin over all 42 days (gray solid line) as well as the TX-Estimate for the periodic intraday (diurnal) component (red dashed line) and the filtered returns (black solid line), whereas panel (b) presents the autocorrelation function of the exemplary stock with its corresponding confidence bounds.*

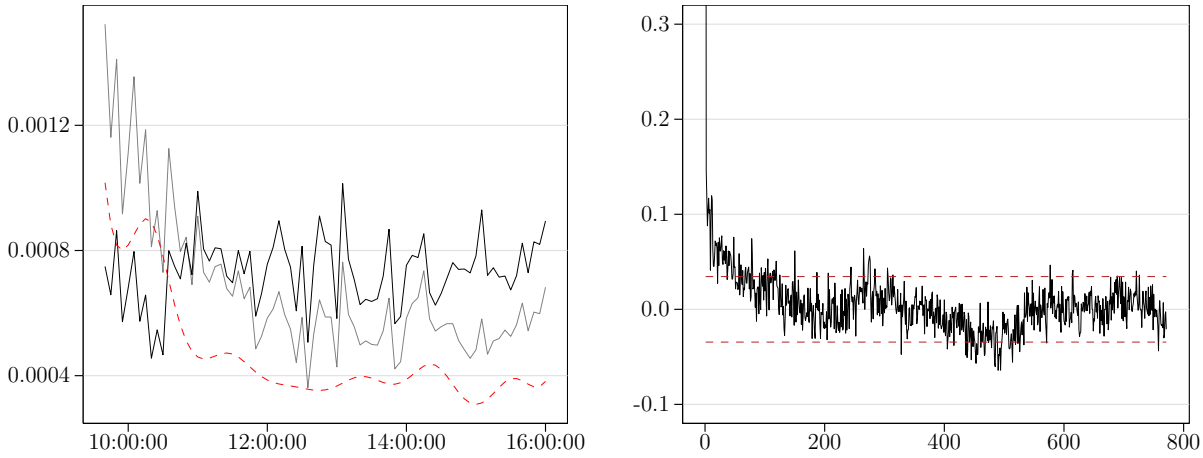

(a) Filtered returns series (b) ACF of filtered returns

Figure 20: Filtered daily average and autocorrelation of absolute returns for *JPM NASDAQ*. *Panel (a) shows the average absolute returns per 5-minute bin over all 42 days (gray solid line) as well as the FFF estimate for the periodic intraday component (red dashed line) and the filtered returns (black solid line), whereas panel (b) presents the autocorrelation function of the exemplary stock with its corresponding confidence bounds.*

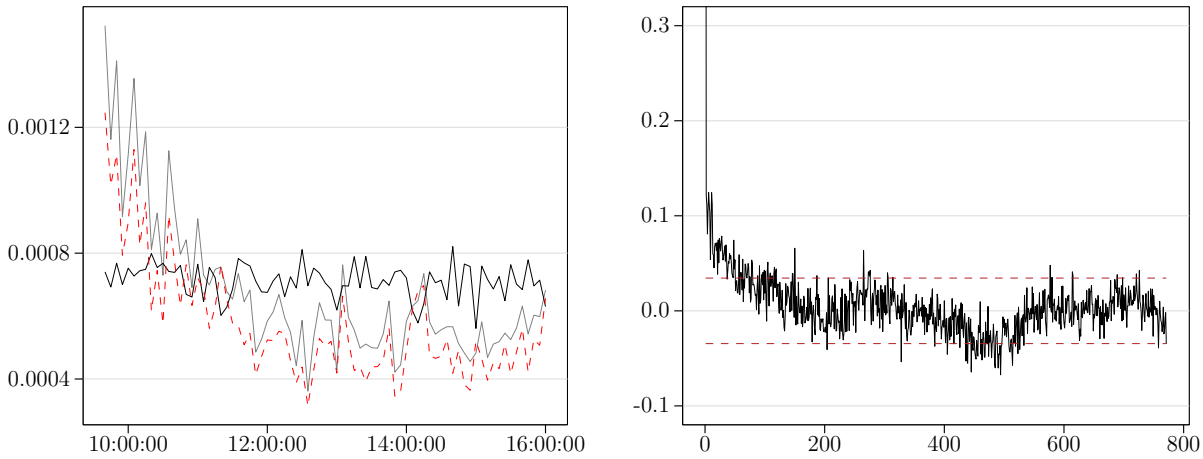

(a) Filtered returns series (b) ACF of filtered returns

Figure 21: Filtered daily average and autocorrelation of absolute returns for *JPM NASDAQ*. *Panel (a) shows the average absolute returns per 5-minute bin over all 42 days (gray solid line) as well as the TX-Estimate for the periodic intraday (diurnal) component (red dashed line) and the filtered returns (black solid line), whereas panel (b) presents the autocorrelation function of the exemplary stock with its corresponding confidence bounds.*

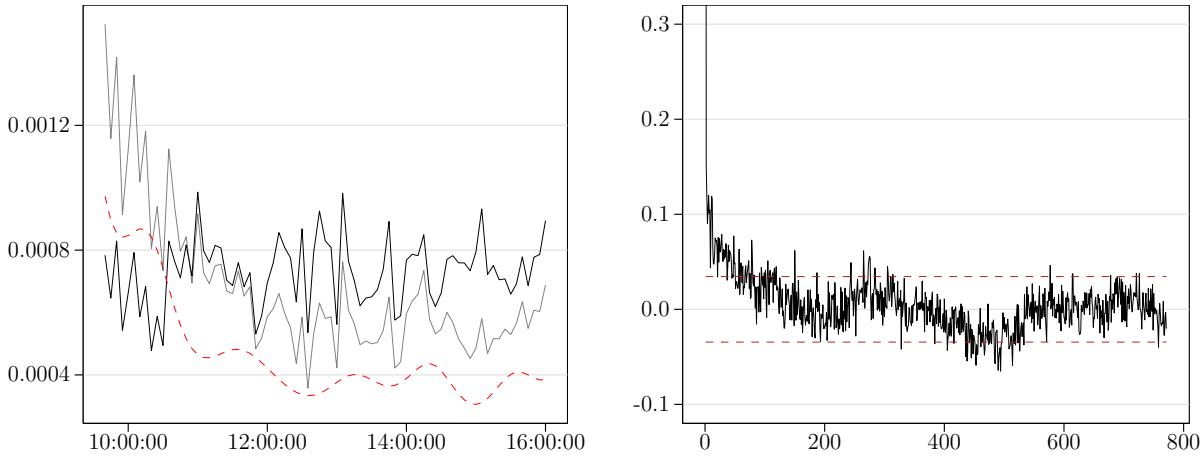

(a) Filtered returns series (b) ACF of filtered returns

Figure 22: Filtered daily average and autocorrelation of absolute returns for *JPM NYSE*. *Panel (a) shows the average absolute returns per 5-minute bin over all 42 days (gray solid line) as well as the FFF estimate for the periodic intraday component (red dashed line) and the filtered returns (black solid line), whereas panel (b) presents the autocorrelation function of the exemplary stock with its corresponding confidence bounds.*

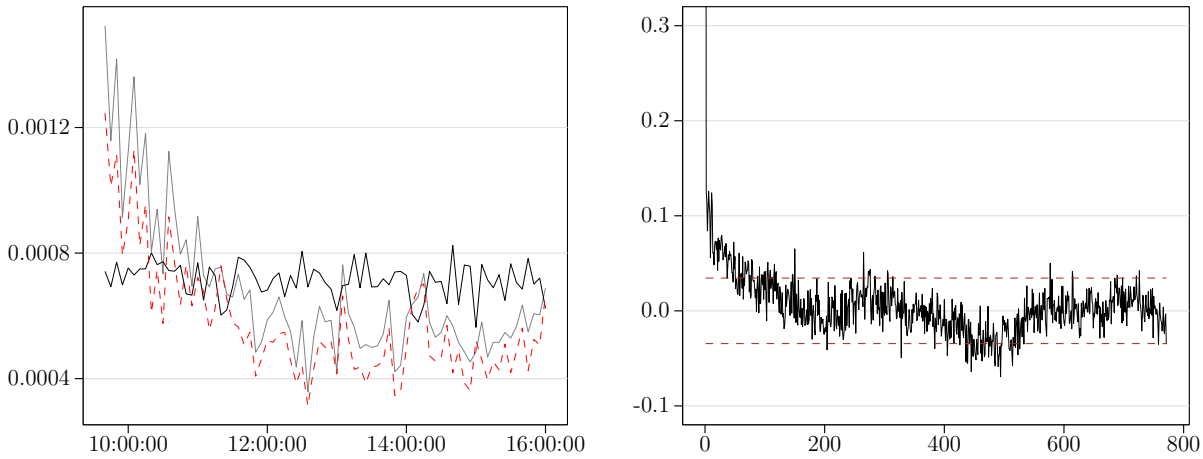

(a) Filtered returns series (b) ACF of filtered returns

Figure 23: Filtered daily average and autocorrelation of absolute returns for *JPM NYSE*. *Panel (a) shows the average absolute returns per 5-minute bin over all 42 days (gray solid line) as well as the TX-Estimate for the periodic intraday (diurnal) component (red dashed line) and the filtered returns (black solid line), whereas panel (b) presents the autocorrelation function of the exemplary stock with its corresponding confidence bounds.*

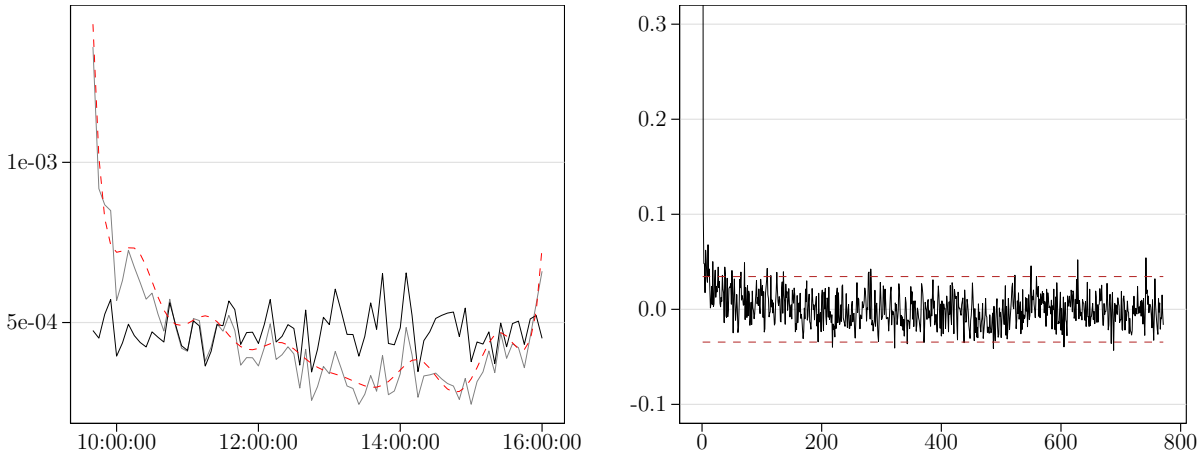

(a) Filtered returns series (b) ACF of filtered returns

Figure 24: Filtered daily average and autocorrelation of absolute returns for *PG NASDAQ*. *Panel (a) shows the average absolute returns per 5-minute bin over all 42 days (gray solid line) as well as the FFF estimate for the periodic intraday component (red dashed line) and the filtered returns (black solid line), whereas panel (b) presents the autocorrelation function of the exemplary stock with its corresponding confidence bounds.*

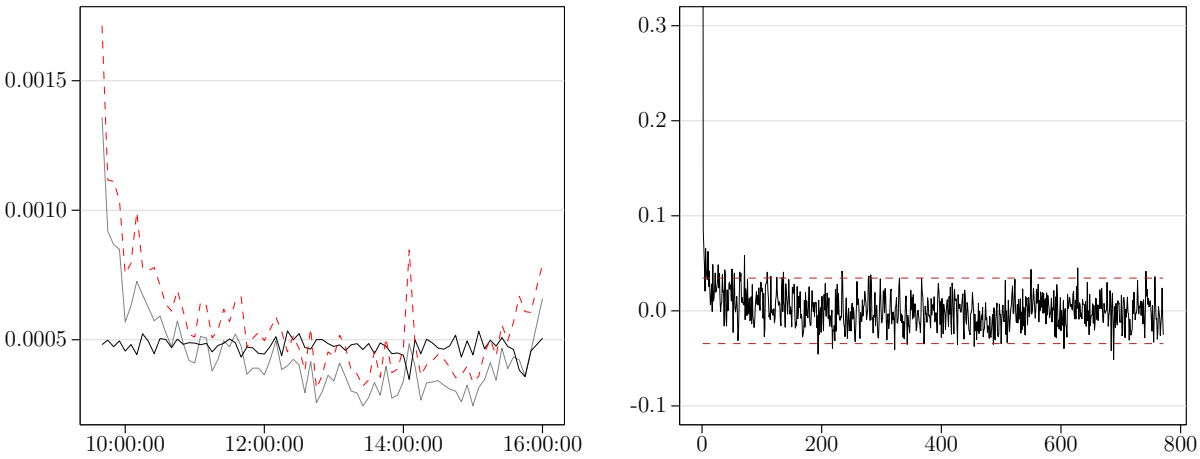

(a) Filtered returns series (b) ACF of filtered returns

Figure 25: Filtered daily average and autocorrelation of absolute returns for *PG NASDAQ*. *Panel (a) shows the average absolute returns per 5-minute bin over all 42 days (gray solid line) as well as the TX-Estimate for the periodic intraday (diurnal) component (red dashed line) and the filtered returns (black solid line), whereas panel (b) presents the autocorrelation function of the exemplary stock with its corresponding confidence bounds.*

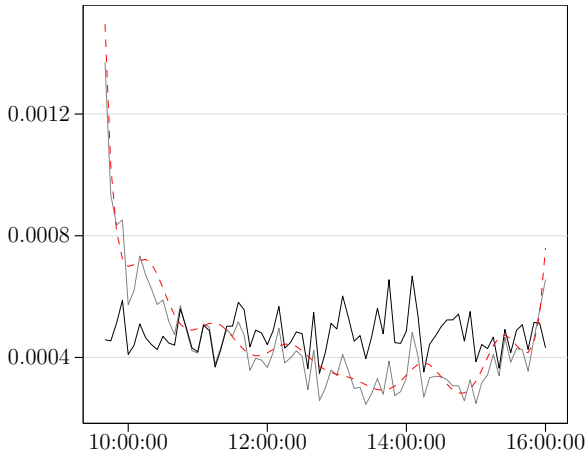

(a) Filtered returns series

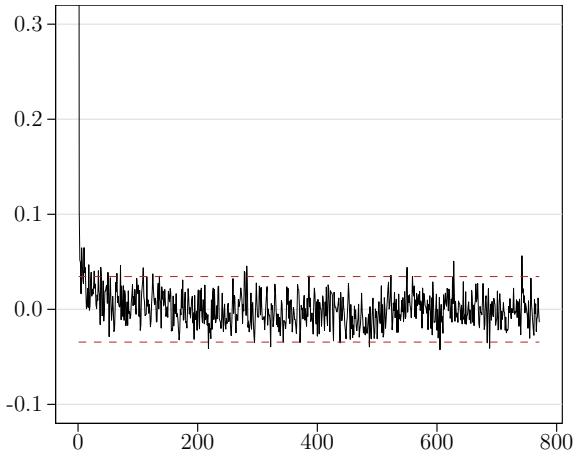

(b) ACF of filtered returns

Figure 26: Filtered daily average and autocorrelation of absolute returns for *PG NYSE*. *Panel (a) shows the average absolute returns per 5-minute bin over all 42 days (gray solid line) as well as the FFF estimate for the periodic intraday component (red dashed line) and the filtered returns (black solid line), whereas panel (b) presents the autocorrelation function of the exemplary stock with its corresponding confidence bounds.*

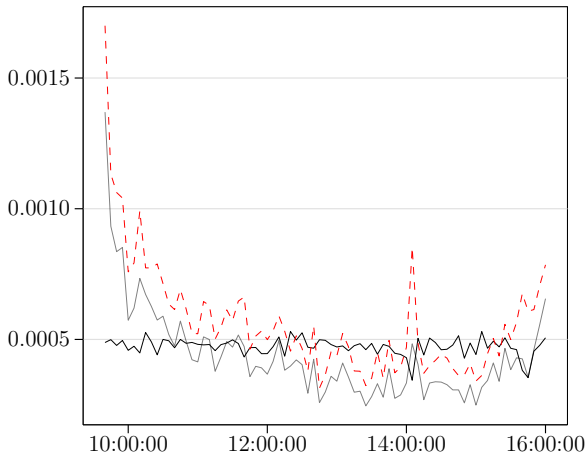

(a) Filtered returns series

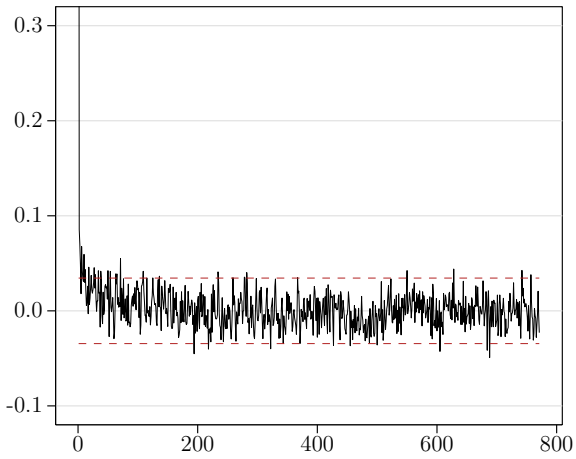

(b) ACF of filtered returns

Figure 27: Filtered daily average and autocorrelation of absolute returns for *PG NYSE*. *Panel (a) shows the average absolute returns per 5-minute bin over all 42 days (gray solid line) as well as the TX-Estimate for the periodic intraday (diurnal) component (red dashed line) and the filtered returns (black solid line), whereas panel (b) presents the autocorrelation function of the exemplary stock with its corresponding confidence bounds.*

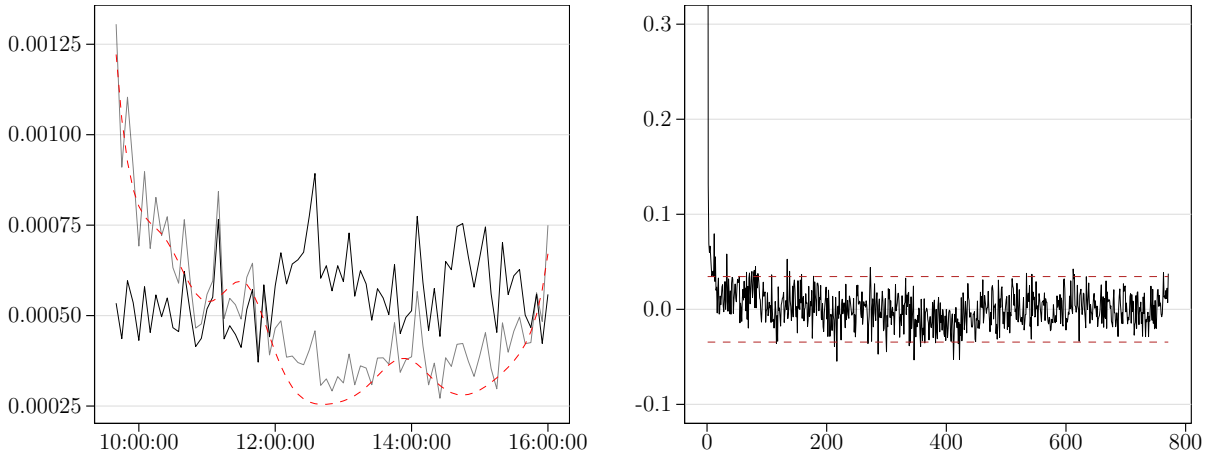

(a) Filtered returns series (b) ACF of filtered returns

Figure 28: Filtered daily average and autocorrelation of absolute returns for *T NASDAQ*. *Panel (a) shows the average absolute returns per 5-minute bin over all 42 days (gray solid line) as well as the FFF estimate for the periodic intraday component (red dashed line) and the filtered returns (black solid line), whereas panel (b) presents the autocorrelation function of the exemplary stock with its corresponding confidence bounds.*

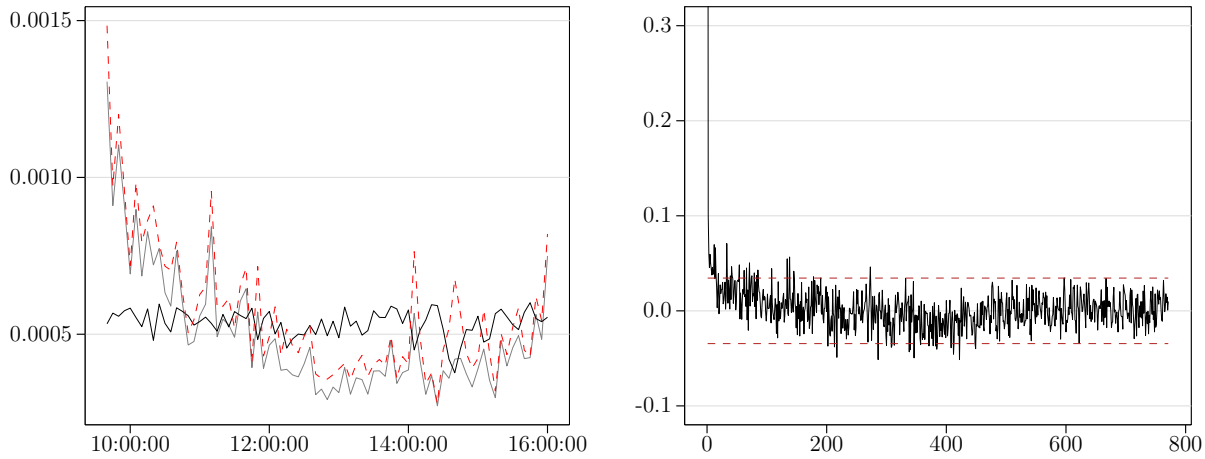

(a) Filtered returns series (b) ACF of filtered returns

Figure 29: Filtered daily average and autocorrelation of absolute returns for *T NASDAQ*. *Panel (a) shows the average absolute returns per 5-minute bin over all 42 days (gray solid line) as well as the TX-Estimate for the periodic intraday (diurnal) component (red dashed line) and the filtered returns (black solid line), whereas panel (b) presents the autocorrelation function of the exemplary stock with its corresponding confidence bounds.*

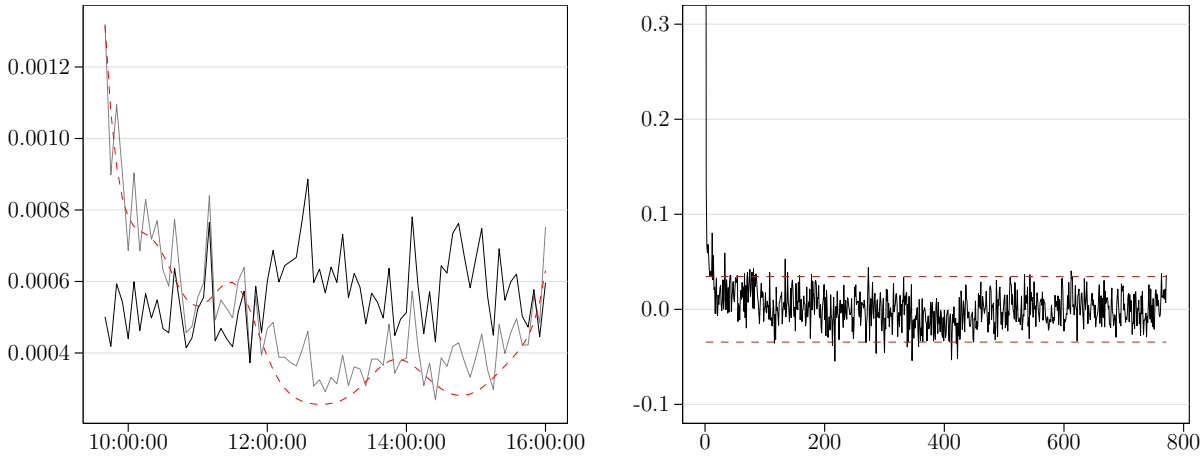

(a) Filtered returns series (b) ACF of filtered returns

Figure 30: Filtered daily average and autocorrelation of absolute returns for *T NYSE*. *Panel (a) shows the average absolute returns per 5-minute bin over all 42 days (gray solid line) as well as the FFF estimate for the periodic intraday component (red dashed line) and the filtered returns (black solid line), whereas panel (b) presents the autocorrelation function of the exemplary stock with its corresponding confidence bounds.*

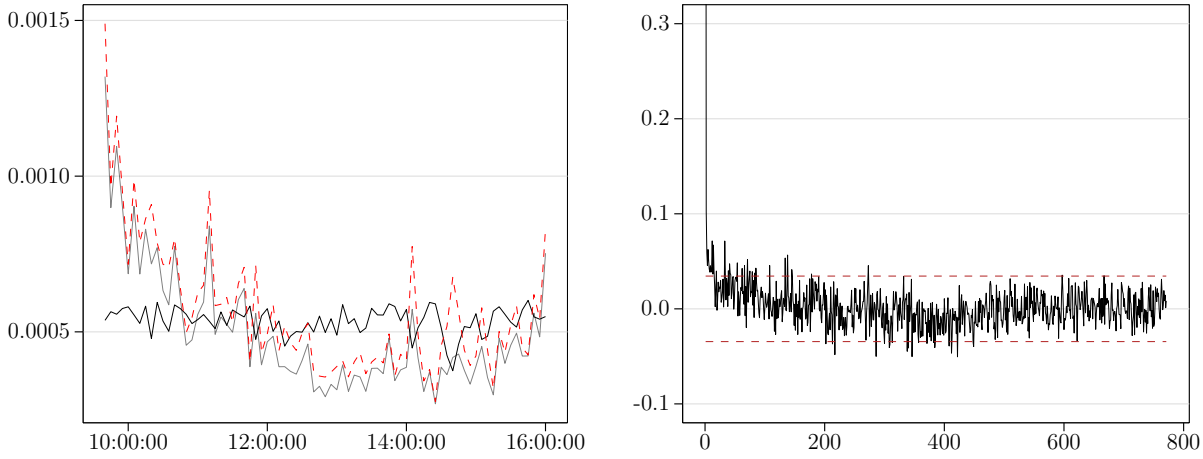

(a) Filtered returns series (b) ACF of filtered returns

Figure 31: Filtered daily average and autocorrelation of absolute returns for *T NYSE*. *Panel (a) shows the average absolute returns per 5-minute bin over all 42 days (gray solid line) as well as the TX-Estimate for the periodic intraday (diurnal) component (red dashed line) and the filtered returns (black solid line), whereas panel (b) presents the autocorrelation function of the exemplary stock with its corresponding confidence bounds.*

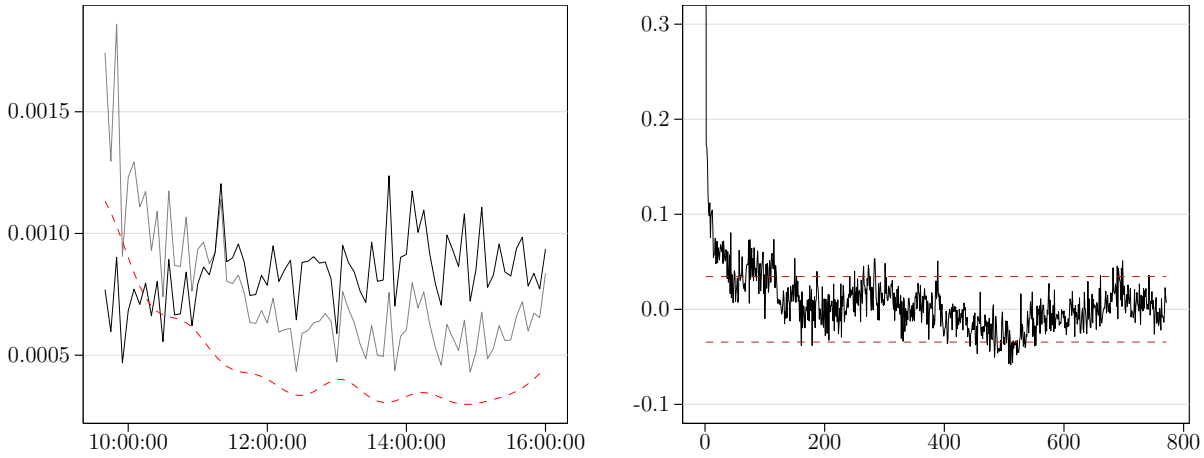

(a) Filtered returns series

(b) ACF of filtered returns

Figure 32: Filtered daily average and autocorrelation of absolute returns for *WFC NASDAQ*. *Panel (a) shows the average absolute returns per 5-minute bin over all 42 days (gray solid line) as well as the FFF estimate for the periodic intraday component (red dashed line) and the filtered returns (black solid line), whereas panel (b) presents the autocorrelation function of the exemplary stock with its corresponding confidence bounds.*

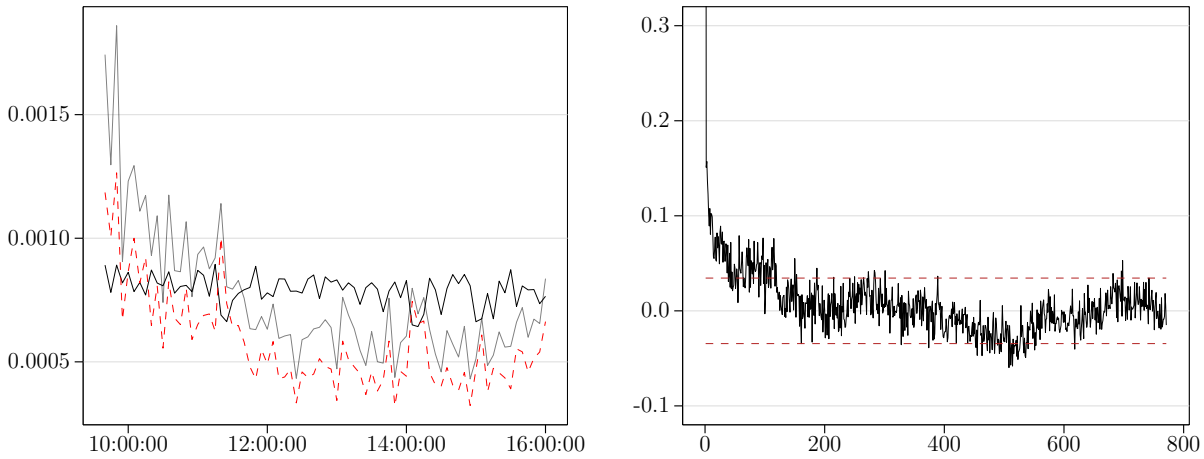

(a) Filtered returns series

(b) ACF of filtered returns

Figure 33: Filtered daily average and autocorrelation of absolute returns for *WFC NASDAQ*. *Panel (a) shows the average absolute returns per 5-minute bin over all 42 days (gray solid line) as well as the TX-Estimate for the periodic intraday (diurnal) component (red dashed line) and the filtered returns (black solid line), whereas panel (b) presents the autocorrelation function of the exemplary stock with its corresponding confidence bounds.*

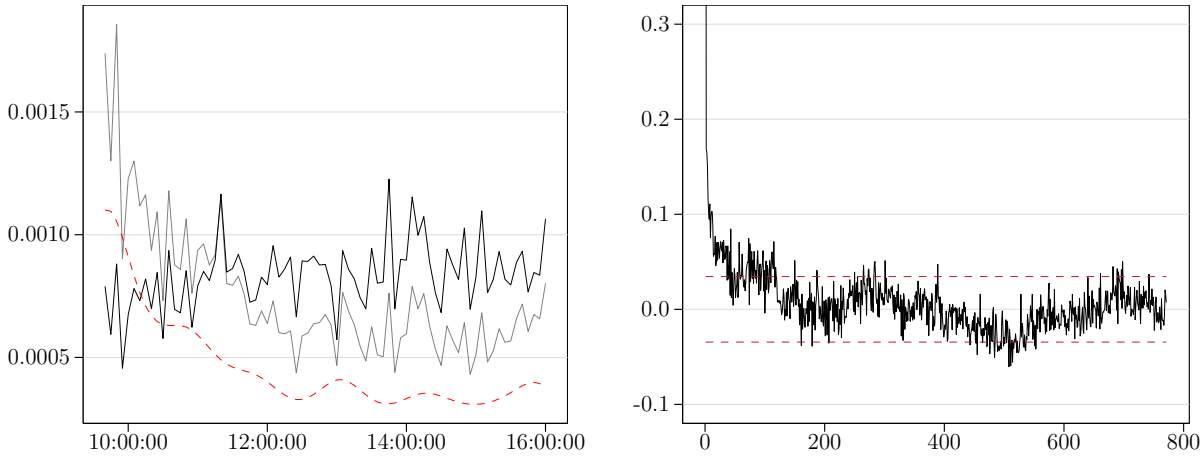

(a) Filtered returns series (b) ACF of filtered returns

Figure 34: Filtered daily average and autocorrelation of absolute returns for *WFC NYSE*. *Panel (a) shows the average absolute returns per 5-minute bin over all 42 days (gray solid line) as well as the FFF estimate for the periodic intraday component (red dashed line) and the filtered returns (black solid line), whereas panel (b) presents the autocorrelation function of the exemplary stock with its corresponding confidence bounds.*

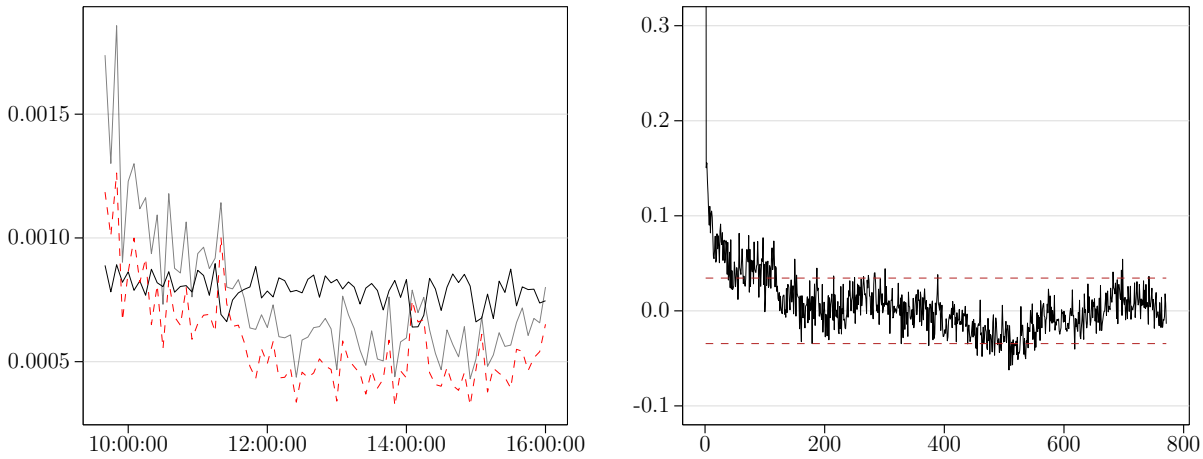

(a) Filtered returns series (b) ACF of filtered returns

Figure 35: Filtered daily average and autocorrelation of absolute returns for *WFC NYSE*. *Panel (a) shows the average absolute returns per 5-minute bin over all 42 days (gray solid line) as well as the TX-Estimate for the periodic intraday (diurnal) component (red dashed line) and the filtered returns (black solid line), whereas panel (b) presents the autocorrelation function of the exemplary stock with its corresponding confidence bounds.*

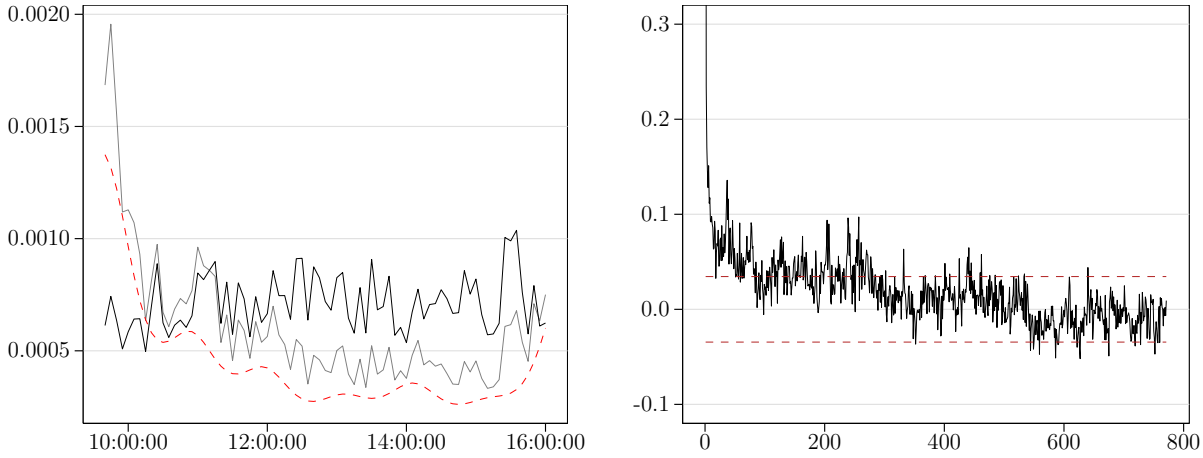

(a) Filtered returns series

(b) ACF of filtered returns

Figure 36: Filtered daily average and autocorrelation of absolute returns for *WMT NASDAQ*. *Panel (a) shows the average absolute returns per 5-minute bin over all 42 days (gray solid line) as well as the FFF estimate for the periodic intraday component (red dashed line) and the filtered returns (black solid line), whereas panel (b) presents the autocorrelation function of the exemplary stock with its corresponding confidence bounds.*

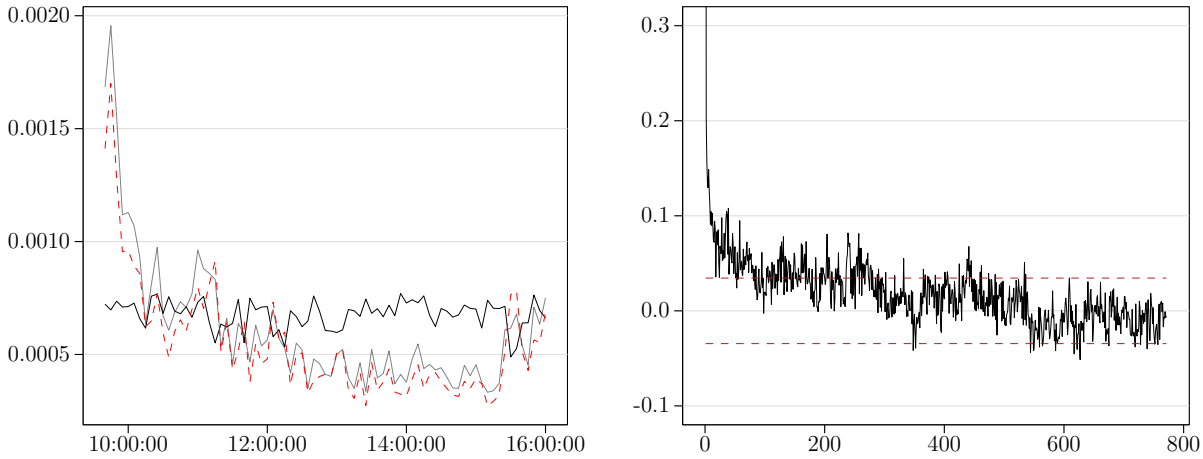

(a) Filtered returns series

(b) ACF of filtered returns

Figure 37: Filtered daily average and autocorrelation of absolute returns for *WMT NASDAQ*. *Panel (a) shows the average absolute returns per 5-minute bin over all 42 days (gray solid line) as well as the TX-Estimate for the periodic intraday (diurnal) component (red dashed line) and the filtered returns (black solid line), whereas panel (b) presents the autocorrelation function of the exemplary stock with its corresponding confidence bounds.*

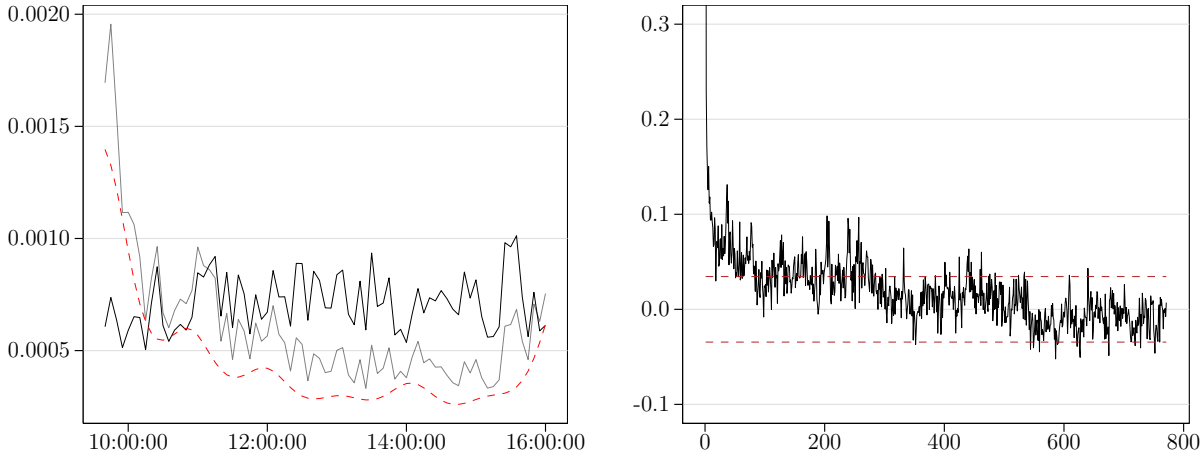

(a) Filtered returns series

(b) ACF of filtered returns

Figure 38: Filtered daily average and autocorrelation of absolute returns for *WMT NYSE*. *Panel (a) shows the average absolute returns per 5-minute bin over all 42 days (gray solid line) as well as the FFF estimate for the periodic intraday component (red dashed line) and the filtered returns (black solid line), whereas panel (b) presents the autocorrelation function of the exemplary stock with its corresponding confidence bounds.*

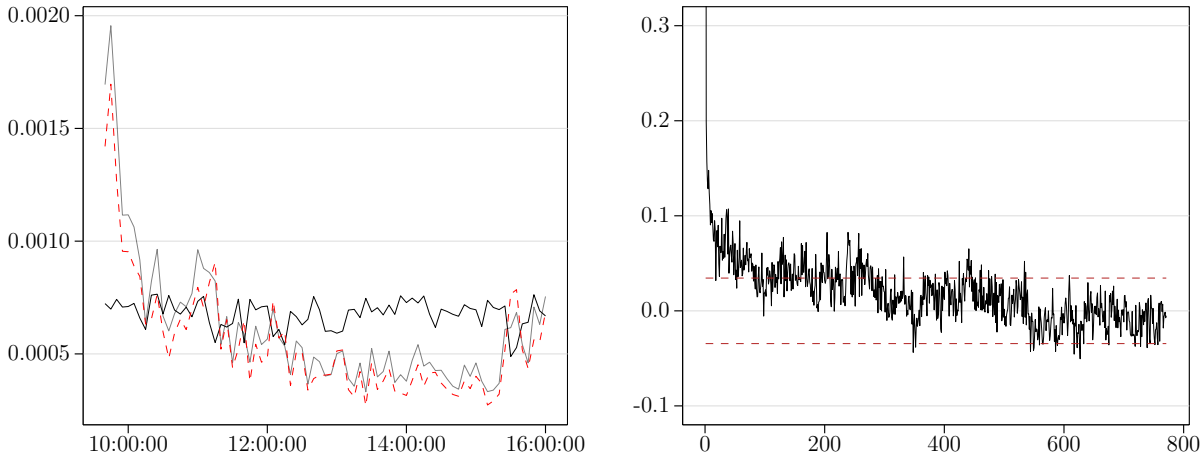

(a) Filtered returns series

(b) ACF of filtered returns

Figure 39: Filtered daily average and autocorrelation of absolute returns for *WMT NYSE*. *Panel (a) shows the average absolute returns per 5-minute bin over all 42 days (gray solid line) as well as the TX-Estimate for the periodic intraday (diurnal) component (red dashed line) and the filtered returns (black solid line), whereas panel (b) presents the autocorrelation function of the exemplary stock with its corresponding confidence bounds.*

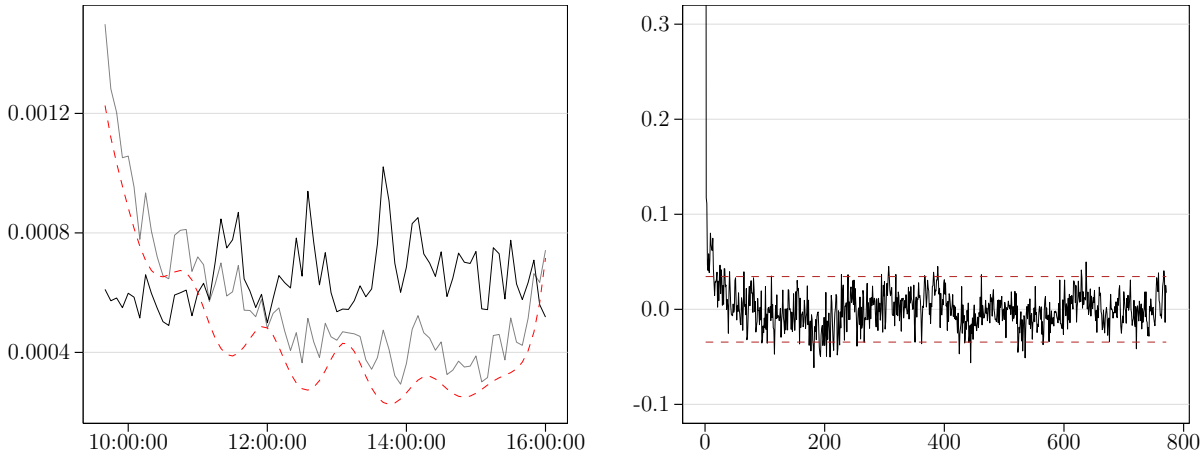

(a) Filtered returns series

(b) ACF of filtered returns

Figure 40: Filtered daily average and autocorrelation of absolute returns for *XOM NASDAQ*. *Panel (a) shows the average absolute returns per 5-minute bin over all 42 days (gray solid line) as well as the FFF estimate for the periodic intraday component (red dashed line) and the filtered returns (black solid line), whereas panel (b) presents the autocorrelation function of the exemplary stock with its corresponding confidence bounds.*

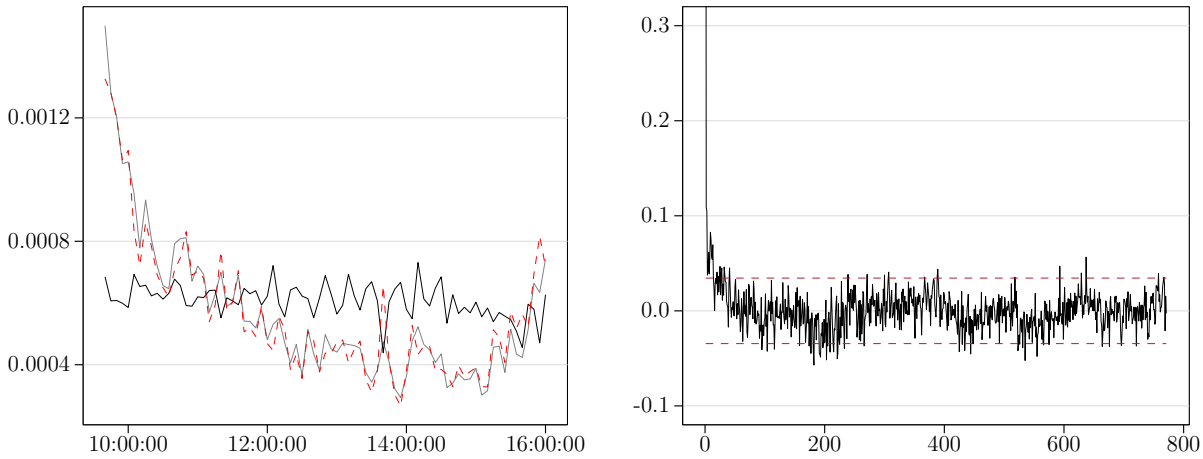

(a) Filtered returns series

(b) ACF of filtered returns

Figure 41: Filtered daily average and autocorrelation of absolute returns for *XOM NASDAQ*. *Panel (a) shows the average absolute returns per 5-minute bin over all 42 days (gray solid line) as well as the TX-Estimate for the periodic intraday (diurnal) component (red dashed line) and the filtered returns (black solid line), whereas panel (b) presents the autocorrelation function of the exemplary stock with its corresponding confidence bounds.*

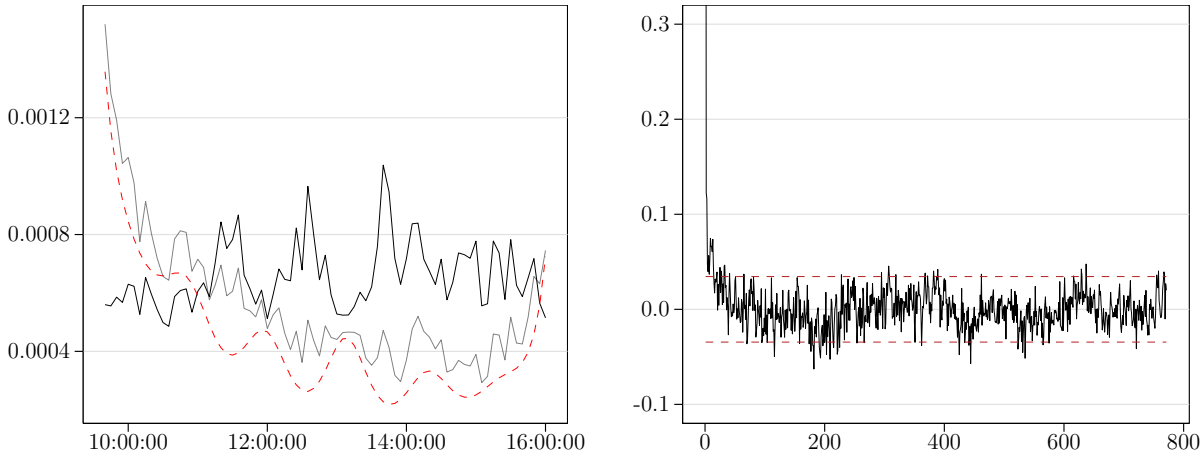

(a) Filtered returns series (b) ACF of filtered returns

Figure 42: Filtered daily average and autocorrelation of absolute returns for *XOM NYSE*. *Panel (a) shows the average absolute returns per 5-minute bin over all 42 days (gray solid line) as well as the FFF estimate for the periodic intraday component (red dashed line) and the filtered returns (black solid line), whereas panel (b) presents the autocorrelation function of the exemplary stock with its corresponding confidence bounds.*

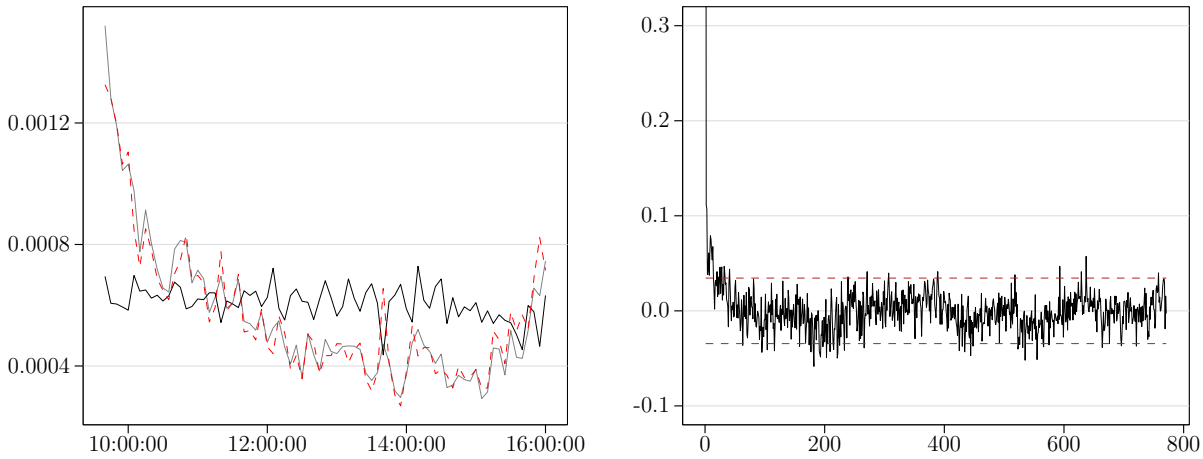

(a) Filtered returns series (b) ACF of filtered returns

Figure 43: Filtered daily average and autocorrelation of absolute returns for *XOM NYSE*. *Panel (a) shows the average absolute returns per 5-minute bin over all 42 days (gray solid line) as well as the TX-Estimate for the periodic intraday (diurnal) component (red dashed line) and the filtered returns (black solid line), whereas panel (b) presents the autocorrelation function of the exemplary stock with its corresponding confidence bounds.*

Authors' Declaration

We hereby declare that the work in this paper was carried out in accordance with the requirements of the university's regulations and that it has not been submitted for any other academic purpose. Except where indicated by specific references in the text, the work is the candidates' own work. Work done in collaboration with, or with the assistance of others, is indicated as such. Any views expressed in the paper are those of the authors.

Martin Haas

Benedikt Schmehr